Distributed formation control for manipulator end-effectors

Wu, Haiwen; Jayawardhana, Bayu; Garcia de Marina, Hector; Xu, Dabo

Published in:
IEEE Transactions on Automatic Control

Distributed formation control for manipulator end-effectors

Haiwen Wu, Bayu Jayawardhana, Hector Garcia de Marina and Dabo Xu

Abstract—**This paper addresses the problem of achieving and maintaining the 2D/3D formation shape of networked manipulator end-effectors. We firstly present a distributed formation controller for manipulators whose system parameters are perfectly known. The formation control objective is achieved by assigning virtual springs between end-effectors and by adding damping terms at joints, which provides a clear physical interpretation of the proposed solution. Subsequently, we extend it to the case where manipulator kinematic and system parameters are not exactly known. An extra integrator and an adaptive estimator are introduced for gravitational compensation and stabilization, respectively. Simulation results with planar manipulators and with seven degree-of-freedom humanoid manipulator arms are presented to illustrate the effectiveness of the proposed approach.**

Index Terms—**Formation control, networked manipulators, end-effector control.**

I. Introduction

This paper investigates the problem of distributed formation control of manipulator end-effectors. Specifically, we consider a group of manipulators whose end-effectors must reach and maintain a prescribed shape in order to fulfill a given group task, such as, collaborative pick-and-place or transportation of large payload, among others. We present distributed control algorithms to solve the problem where the popular gradient-descent formation control for single integrator agents is combined with a passivity-based manipulator controller in the task-space.

The use of coordinated manipulators or mobile manipulators[1] have been developed and deployed in smart manufacturing and logistics systems for the past decades. In these application areas, maintaining a robust formation of robots is important, in particular, when they are used to transport large payloads where slight deformation on the formation can be hazardous. In this context, distributed formation controllers can be deployed to the group of robots where each robot uses local on-board sensor systems to maintain formation shape constraints that are defined between the robot and its neighbors [1], [2]. When the agent is considered as a kinematic point (or point mass) whose dynamics is given by single-integrators and double-integrators, fundamental gradient-based control laws have been proposed and studied, for instance, in [3], [4], [5], [6], [7] where different sources of local information (relative position, distance, bearing or vision) are used. The extension of the formation control to other classes of nonlinear systems includes the formation of non-holonomic wheeled robots [8], [9], spacecraft formation flying [10], [11], and dynamic positioning of multiple offshore vessels [12]. In all of these works, the control input acts directly on the state variables that define the formation. It remains an open problem on the design of formation control for systems where the control input does not act directly on the formation error variables, such as, the formation control of underactuated systems or end-effector manipulator systems as studied in this paper.

For the latter case, where we are dealing with the formation control problem for end-effectors, the desired formation shape is defined by the end-effectors' position while the control inputs or the actuators act at the joints' level, which makes this problem more challenging. One can consider two level of controllers where distributed formation control law is designed for the formation keeping of end-effectors as kinematic points, and subsequently, the computed velocity at each end-effector for maintaining the formation is back-propagated to the control inputs at the joints' level via inverse kinematics. This multi-level control scheme is, in practice, non-trivial since there is no time-scale separation in the use of collaborative manipulators for high-speed robotization in industry, and the computation of inverse kinematics is computationally demanding.

We start with presenting a gradient-based distributed control design for manipulators whose system parameters are perfectly known based only on local information, and where the desired formation shape can be made exponentially stable. The proposed controller is composed of the use of virtual springs between the end-effectors and damping terms at the joints. Such physics-based control design approach allows us to obtain physical interpretation of the proposed approach. The virtual springs embody the generalization of gradient-based distributed formation control law from the single-integrator agents to the robotic manipulator ones where the distributed control forces for the end-effectors in order to reach and to maintain the formation are distributed to the control forces at each joint.

Subsequently, we extend the gradient-based control law to the case where the manipulator kinematic and dynamic parameters are not exactly known. Based on the internal model principle, an additional integrator is introduced for

Haiwen Wu and Bayu Jayawardhana are with Engineering and Technology Institute Groningen, Faculty of Science and Engineering, University of Groningen, Groningen 9747 AG, The Netherlands (e-mails: haiwen.wu@rug.nl; b.jayawardhana@rug.nl). H.G. de Marina is with Department of Computer Engineering, Automation and Robotics, Universidad de Granada and CITIC, Spain (email: hgdemarina@ugr.es). The work of H.G. de Marina is supported by the grant Ramon y Cajal RYC2020-030090-I from the Spanish Ministry of Science. Dabo Xu is with the School of Automation, Nanjing University of Science and Technology, Nanjing 210094, China (e-mail: dxu@njust.edu.cn). The work of D. Xu is supported by National Natural Science Foundation of China under Grant No. 62073168.

[1]Mobile manipulators refer to mobile robots where manipulator arms are mounted on the mobile platform.

gravitational compensation in dealing with uncertainties in the forces coming from the potential energy. To handle uncertainties relating to the kinematics, we present firstly a controller design using nominal (approximate) Jacobian. A sufficient condition is given to show that the desired shape can be made exponentially stable if the mismatch between the nominal Jacobian and the actual Jacobian is bounded by a known constant. Based on that, we propose an adaptive Jacobian controller which removes the bounded mismatch condition. Our proposed distributed formation control law uses local information that comes from the on-board sensor systems defined on local coordinate frame. In other words, the relative information of an end-effector's position with respect to its neighbors and the joints' position/velocity of the robot is independent of its neighbors' frames.

The rest of this paper is organized as follows. In Section II, we present system models, some preliminaries on formation graph and problem formulation. Our first gradient-based controller for manipulators whose system parameters are exactly known with stability analysis for closed-loop systems is discussed in Section III. In Section IV, the extension of the aforementioned gradient-based controller for manipulators with kinematic and dynamic uncertainties is presented. It is followed by further discussions in Section V. For illustrating the efficacy of our proposed distributed formation control approaches, we show numerical examples in Section VI. Concluding remarks are given in Section VII.

II. Preliminaries and Problem Formulation

Notation. We denote by $\mathbb{R}_{>0}$ the set of all positive real numbers. $\|\cdot\|$ is the Euclidean norm in $\mathbb{R}^n$ or the induced matrix 2-norm in $\mathbb{R}^{n\times m}$. For a matrix $A \in \mathbb{R}^{m\times n}$, A^T denotes its transpose, $\lambda_{\min}\{A\}$ and $\lambda_{\max}\{A\}$ denote the minimum and maximum eigenvalue of matrix A, respectively. For column vectors $x_1,\dots,x_n$, we write $\mathrm{col}(x_1,\dots,x_n) := [x_1^T,\dots,x_n^T]^T$ as the stacked column vector. We will denote by $\otimes$ the Kronecker product, and we will use a shorthand notation $\overline{B} := B\otimes I_m$ for any $B\in\mathbb{R}^{n\times m}$ and identity matrix I_m of dimension m.

A. Manipulator dynamics and kinematics

Consider a group of n-DOF fully-actuated rigid robotic manipulator modeled by [13], [14], [15]

$$H_i(q_i,w_i)\ddot{q}_i + C_i(q_i,\dot{q}_i,w_i)\dot{q}_i + G_i(q_i,w_i) = u_i \tag{1}$$

where $i\in\{1,\dots,N\}$, where $q_i(t),\dot{q}_i(t),\ddot{q}_i(t)\in\mathbb{R}^n$ are the generalized joint position, velocity, and acceleration, respectively, $u_i(t)\in\mathbb{R}^n$ is the generalized joint control forces, $w_i\in\mathbb{W}_i\subset\mathbb{R}^{n_w}$ is the constant system parameter vector for known bounded compact set $\mathbb{W}_i$, $H_i(q_i,w_i)\in\mathbb{R}^{n\times n}$ is the inertia matrix, $C_i(q_i,\dot{q}_i,w_i)\in\mathbb{R}^{n\times n}$ is the Coriolis and centrifugal force matrix-valued function, and $G_i(q_i,w_i)\in\mathbb{R}^n$ is the gravitational torque.

Let $x_i(t)\in\mathbb{R}^m$ be the ith manipulator end-effector position in the task-space (e.g., Cartesian space with $m\in\{2,3\}$) with respect to the world frame Σ_g and $m\le n$. The end-effector position can be mapped to its generalized joint position via a nonlinear forward kinematics mapping [14], [15]

$$x_i = h_i(q_i,w_i) + x_{i0} \tag{2}$$

where $h_i:\mathbb{R}^n\times\mathbb{R}^{n_w}\to\mathbb{R}^m$ is the mapping from joint-space to task-space, and $x_{i0}\in\mathbb{R}^m$ is the position of manipulator base with respect to the world frame Σ_g.

Differentiating (2) with respect to time gives the relation between the task-space velocity and joint velocity [14, pp. 196], [15, pp. 122]

$$\dot{x}_i = J_{g,i}(q_i,w_i)\dot{q}_i,\quad J_{g,i}(q_i,w_i) := \frac{\partial h_i(q_i,w_i)}{\partial q_i} \tag{3}$$

where $J_{g,i}(q_i,w_i)\in\mathbb{R}^{m\times n}$ is called the Jacobian matrix of the forward kinematics.

The present study focuses on manipulators with fixed bases. Suppose all the manipulators are suitably prepositioned such that their *working spaces* are disjoint. Regarding the kinematic singularities, let

$$\mathbf{Q}_{w_i} := \{q_i\in\mathbb{R}^n : \dim\big(\mathrm{null}(J_{g,i}(q_i,w_i))\big) = 0\}$$

for all $w_i\in\mathbb{W}_i$, denote the set of generalized joint positions that is free of kinematic singularities. Within this set, for each manipulator (with system parameter w_i and base position x_{i0}), we define

$$\mathcal{W}_i := \{x_i\in\mathbb{R}^m : x_i = h_i(q_i,w_i)+x_{i0},\ q_i\in\mathbf{Q}_{w_i}\}$$

for all $w_i\in\mathbb{W}_i$, as a subset of its reachable *working spaces*. The entire reachable *working space* for the networked manipulators can be given by

$$\mathcal{W} := \mathcal{W}_1\times\cdots\times\mathcal{W}_N.$$

Throughout this paper, we assume standard properties on the inertia and Coriolis matrices H_i and C_i that are commonly inherited in most Euler-Lagrange systems [16], [17]. In particular, we assume the following properties.

P1 The inertia matrix $H_i(q_i,w_i)$ is positive definite. More specifically, there are known constants $c_{i,\min},c_{i,\max}>0$ such that

$$c_{i,\min}I_n \le H_i(q_i,w_i) \le c_{i,\max}I_n,\quad \forall q_i\in\mathbb{R}^n, w_i\in\mathbb{W}.$$

P2 The matrix-valued function $\dot{H}_i(q_i,\dot{q}_i,w_i) - 2C_i(q_i,\dot{q}_i,w_i)$ is skew symmetric, i.e., for any differentiable function $q_i(t)\in\mathbb{R}^n$ and its time derivative $\dot{q}_i(t)$,

$$\dot{H}_i(q_i,\dot{q}_i,w_i) = C_i(q_i,\dot{q}_i,w_i) + C_i^T(q_i,\dot{q}_i,w_i) \tag{4}$$

where $\dot{H}_i(q_i,\dot{q}_i,w_i) = \sum_{j=1}^n \frac{\partial H_i}{\partial q_{ij}}\dot{q}_{ij}$.

P3 The velocity kinematics (3) linearly depends on a kinematic parameter vector $a(w)\in\mathbb{R}^p$, i.e., there are smooth functions $a_i(\cdot)\in\mathbb{R}^p$ and $Z_i(\cdot)\in\mathbb{R}^{m\times p}$ such that for any vectors $q_i(t)\in\mathbb{R}^n$, $\zeta_i(t)\in\mathbb{R}^m$,

$$J_{g,i}^T(q_i,w_i)\zeta_i = Z_i(q_i,\zeta_i)a_i(w_i) \tag{5}$$

where $Z_i(\cdot)$ is referred to as a *kinematic regressor matrix* to be known. Moreover, there is a smooth matrix-valued function $J_i:\mathbb{R}^n\times\mathbb{R}^p\to\mathbb{R}^{m\times n}$ such that

$$J_i(q_i,a_i) = J_{g,i}(q_i,w_i),\quad a_i := a_i(w_i) \tag{6}$$

and consequently

$$J_i^T(q_i, a_i)\zeta_i = J_{g,i}^T(q_i, w_i)\zeta_i = Z_i(q_i, \zeta_i)a_i.$$

B. Graph on formation

Let $1 < N \in \mathbb{N}$ define the number of robotic manipulators whose end-effectors must maintain a specific formation. The neighboring relationships between their end-effectors are described by an undirected and connected graph $\mathcal{G} := \{\mathcal{V}, \mathcal{E}\}$ with the vertex set $\mathcal{V} := \{1, \cdots, N\}$ and the ordered edge set $\mathcal{E} \subset \mathcal{V} \times \mathcal{V}$. The set of the neighbors for the end-effector i is given by $\mathcal{N}_i := \{j \in \mathcal{V} : (i, j) \in \mathcal{E}\}$. We use $|\mathcal{V}| = N$ and $|\mathcal{E}|$ to denote the number of vertices and edges of $\mathcal{G}$, respectively. We define the elements of the incidence matrix $B \in \mathbb{R}^{|\mathcal{V}| \times |\mathcal{E}|}$ of $\mathcal{G}$ by

$$b_{ik} = \begin{cases} +1, & i = \mathcal{E}_k^{\text{tail}} \\ -1, & i = \mathcal{E}_k^{\text{head}} \\ 0, & \text{otherwise} \end{cases}$$

where $\mathcal{E}_k^{\text{tail}}$ and $\mathcal{E}_k^{\text{head}}$ denote the tail and head nodes, respectively, of the edge $\mathcal{E}_k$, i.e., $\mathcal{E}_k = (\mathcal{E}_k^{\text{tail}}, \mathcal{E}_k^{\text{head}})$. Note that $B^T \mathbf{1}_{|\mathcal{V}|} = 0$, where $\mathbf{1}_n \in \mathbb{R}^n$ is the vector with all its entries to be ones.

C. End-effector distributed formation control problem

We refer to *configuration* as the stacked vector of end-effectors' positions $x = \text{col}(x_1, \dots, x_N) \in \mathbb{R}^{mN}$, and we refer to *framework* as the pair $(\mathcal{G}, x)$. Given a *reference configuration* x^*, we define the *desired shape* as the set

$$\mathcal{S} := \{x : x = (I_N \otimes R)x^* + \mathbf{1}_N \otimes b,\ R \in \text{SO}(m), b \in \mathbb{R}^m\}. \tag{7}$$

Let us stack all joint coordinates into $q = \text{col}(q_1, \dots, q_N)$ and $\dot{q} = \text{col}(\dot{q}_1, \dots, \dot{q}_N)$. Note that $\mathcal{S}$ accounts for any arbitrary translation and rotation. However, the *working space* for the end-effectors is constrained since we assume that the bases of the arm manipulators are fixed. Therefore, we define $\mathcal{S}_W = \mathcal{S} \cap \mathcal{W}$ as the subset of shapes that are both desired and reachable by the end-effectors. An illustrative example showing the relationship between $\mathcal{S}$ and $\mathcal{S}_W$ is given in Fig. 1.

We are now ready to formulate our formation control problem of end-effectors as follows.

Problem 2.1: (End-effector distributed formation control problem). For a group of N manipulators given by (1), whose end-effector positions are as in (2), design a distributed control law of the form

$$\begin{cases} \dot{\chi}_i = f_{ci}\Big((x_i - x_j)_{j \in \mathcal{N}_i}, q_i, \dot{q}_i, \chi_i\Big) \\ u_i = h_{ci}\Big((x_i - x_j)_{j \in \mathcal{N}_i}, q_i, \dot{q}_i, \chi_i\Big) \end{cases} \tag{8}$$

where, for each $i \in \{1, \dots, N\}$,

$$(x_i - x_j)_{j \in \mathcal{N}_i} := \text{col}_{j \in \mathcal{N}_i}(\dots, x_i - x_j, \dots)$$

such that $x(t) \to \mathcal{S}_W$ and $\dot{q}(t) \to \mathbf{0}$ as $t \to \infty$ for all initial states $(x(0), \xi(0))$ in a neighborhood of $\mathcal{S}_W \times \mathbf{0}$ and away from kinematic singularities.

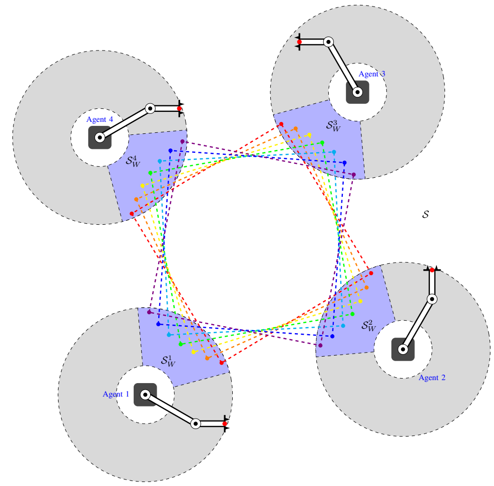

Fig. 1. End-effector formation of 4 two-link planar manipulators (whose working space are the gray rings) in the horizontal plane. The desired shape $\mathcal{S}$ ranges in the whole horizontal plane. The reachable desired set $\mathcal{S}_W = \mathcal{S}_W^1 \times \mathcal{S}_W^2 \times \mathcal{S}_W^3 \times \mathcal{S}_W^4$ is the intersection of $\mathcal{S}$ and working space. The dotted squares (in rainbow colors) are possible reachable desired formations.

In what follows, we will focus on the distributed control design framework where we can directly extend the well-known distributed formation control of mobile robots (modeled as single-integrator agents) to the formation control of end-effectors in arm manipulators. In the latter case, the dynamics is given by second-order systems as in (1) while the control input is defined at the joint level. In order to illustrate our design framework, we consider the use of displacement-based [18] and distance-based formation control [19], both of which are fundamental and popular in distributed control methods. We note that our proposed framework is extensible to other gradient-descent based approaches, such as those that are based on the bearing-rigidity framework [7].

For the displacement-based formation control, we have that $R = I_m$ in (7). In other words, it only admits desired formation shapes which are given by the translation of x^*. On the other hand, the distance-based formation control admits desired formation shapes that are both the translation and rotation of x^*.

The shape displayed by the reference configuration x^* can also be described by a set of geometric relations between the neighboring end-effectors. If $\mathcal{G}$ is connected, then the relative positions defined by the graph $z^* = \overline{B}^T x^*$ define uniquely the desired shape in displacement-based control, i.e., we have the singleton $\mathcal{Z}_{\text{displacement}} := \{z : z = z^*\}$. Note that the elements of z^* correspond to the ordered $z_{ij}^* = z_k^* := x_i^* - x_j^*$, $(i, j) = \mathcal{E}_k \in \mathcal{E}$. If $\mathcal{G}$ is infinitesimally and minimally rigid (e.g., it has a minimum number of edges for being infinitesimally rigid [20]), then the set of distances $\|z_{ij}^*\|, (i, j) \in \mathcal{E}$ define locally[2] the desired shape, i.e., we have the set $\mathcal{Z}_{\text{distance}} := \{z : \|z_{ij}\| = \|x_i - x_j\|,\ (i, j) \in \mathcal{E}\}$.

There are some advantages and disadvantages between the use of displacement-based and distance-based formation control. The former requires a minimum number of edges for

[2]In the sense that it might define a finite number of other shapes.

$\mathcal{G}$, and the resultant control action for pure kinematic agents is linear. However, the desired shape can only be a translation version of x^*, and the algorithm requires neighboring agents to share the same frame of coordinates to control the common vector z_{ij}^*. On the other hand, the distance-based formation control requires more edges, e.g., at least $(2N-3)$ in 2D, and the control action for pure kinematic agents is nonlinear leading to only local stability around $\mathcal{S}$. Nevertheless, it allows a more flexible $\mathcal{S}$, e.g., it allows rotations for x^* and the agents do not need to share a common frame of coordinates since they are controlling the scalars $\|z_{ij}^*\|$.

Remark 2.1: Industrial manipulators use commonly a spherical wrist at the end-effector, and therefore they can achieve any desired orientation at a given end-effector's position [14, pp. 95]. This allows us to focus only on the position of the end-effector since its orientation is *decoupled* thanks to the spherical wrist.

III. Gradient-based Control Design

In this section, we propose a distributed control design framework for the case where all the system parameters are exactly known. A preliminary result is also presented on our previous work [21]. There are two main elements for each controller u_i: an end-effector formation controller u_i^f, and a joint velocity controller u_i^v. In Section III-A, we design control law u_i^f by using virtual springs, and design u_i^v based on the passivity property between joint torque and joint velocity. The whole controller is the sum of the parts. Then in Section III-B, we present stability and convergence analysis of the overall closed-loop system.

Generally speaking, for solving Problem 2.1, we firstly employ the virtual spring approach to the end-effectors and introduce standard distributed formation controllers that are based on gradient-descent approach. The virtual couplings shapes the energy function of the network whose minima are equilibrium points associated to the desired formation shape. If all of the couplings of the network reach their minimum potential energy, the desired formation is reached. The resulting distributed formation control law defined in the end-effector space is propagated to the joint-space via passivity-based approach.

A. Gradient control

To achieve the desired formation shape, we start by assigning virtual springs [22, Chapter 12.2] on the undirected graph $\mathcal{G}$ of the end-effectors, as depicted in Fig. 2. That is, each edge of $\mathcal{E}$ between the manipulators end-effectors are interconnected by virtual couplings that shape the energy function of the network. The network's energy function is designed such that its minima are equilibrium points associated to the desired formation shape.

Consider the k-th edge between agents i and j connected with a virtual coupling. Let us define the following error signal for each edge k of $\mathcal{G}$

$$e_k(t) := f_e(z_k(t), z_k^*) \tag{9}$$

where $f_e : \mathbb{R}^m \to \mathbb{R}^l$, and $l \in \mathbb{N}$ will depend on the chosen formation control strategy, e.g., $f_e = \|z_k\|^2 - \|z_k^*\|^2$ for the distance-based formation control, and $f_e = z_k - z_k^*$ for the displacement-based formation control. Each end-effector in the edge $\mathcal{E}_k = (i,j)$ will subsequently use the gradient descent of $V_k(e_k) = \frac{1}{2}\|e_k\|^2$ as its control input (e.g., its velocity when it is described by kinematic point) in order to reach the minimum of V that coincides with the desired shape. It can be checked that the following equality $\nabla_{x_i} V_k = -\nabla_{x_j} V_k \in \mathbb{R}^m$ is satisfied since $z_{ij} = x_i - x_j$. Let us stack all the e_k in $e \in \mathbb{R}^{l|\mathcal{E}|}$ and define

$$V(e) := \sum_{k=1}^{|\mathcal{E}|} V_k(e_k)$$

For compact representation, we define the m-dimensional agent-wise displacement measurement $\widehat{e}_i(t) \in \mathbb{R}^m$, $i = 1, \ldots, N$ by

$$\widehat{e}_i := \nabla_{x_i} V(e) \tag{10}$$

or equivalently

$$\widehat{e}_i := \sum_{k=1}^{|\mathcal{E}|} b_{ik} R_k(z_k) e_k \text{ with } R_k(z_k) = \frac{\partial f_e(z_k, z_k^*)}{\partial z_k}.$$

In the above, for the displacement-based formation control: $R_k(z_k) = I_m$ and for the distance-based one: $R_k(z_k) = 2z_k$.

Since the virtual springs are assigned between end-effectors, while the actuators are embedded in joints, the corresponding formation control law u_i^f of agent i can be written as

$$u_i^f = -K_P J_i^T(q_i, a_i) \nabla_{x_i} V(e) = -K_P J_i^T(q_i, a_i) \widehat{e}_i \tag{11}$$

with design parameter $K_P \in \mathbb{R}_{>0}$, where $J_i(q_i, a_i)$ is the manipulator Jacobian matrix and $\widehat{e}_i$ is defined in (10).

Let us stack all the $\widehat{e}_i$ in $\widehat{e} \in \mathbb{R}^{mN}$, so that we can write it in the following compact form $\widehat{e} = \nabla_x V$. More precisely, for the displacement-based and for the distance-based ones, we have

$$\widehat{e}_{\text{displacement}} = \nabla_x V_{\text{displacement-based}} = \overline{B} e_{\text{displacement}} \tag{12}$$

$$\widehat{e}_{\text{distance}} = \nabla_x V_{\text{distance-based}} = 2\overline{B} D_z e_{\text{distance}} \tag{13}$$

where $D_z = \text{block diag}(z_1, \ldots, z_{|\mathcal{E}|})$.

We note two relevant facts that will be useful for our main technical results. First, $B^T B$ is positive definite if $\mathcal{G}$ does not contain any cycles. Second, $D_z^T \overline{B^T B} D_z$ is positive definite if $\mathcal{G}$ is infinitesimally and minimally rigid. Roughly speaking, infinitesimally rigid means that all the positions x_i are in a generic configuration, e.g., they are not collinear if $m = 2$ or coplanar if $m = 3$. Note that if the formation is infinitesimally rigid at $\mathcal{S}$, then it is a neighborhood of $\mathcal{S}$ as well.

Next, for solving the static formation control problem, we proceed by designing a control law to stabilize the joint velocity at origin. Let us define

$$\xi_i(t) := \dot{q}_i(t). \tag{14}$$

According to the well-known passivity of manipulators from joint torque to joint velocity [15], we introduce the following controller, consisting of a damping term and a gravity compensation term

$$u_i^v = -K_D \xi_i + G_i(q_i, w_i) \tag{15}$$

with design parameter $K_D \in \mathbb{R}_{>0}$.

B. Closed-loop system

In this part, we will combine the individual control laws u_i^f and u_i^v above and analyze the solvability of Problem 2.1. Before presenting the following main result, for the rest of the paper and for the sake of presentation convenience, we denote: $c_{\min} = \min_{i\in\{1,\ldots,N\}}\{c_{i,\min}\}$, $c_{\max} = \max_{i\in\{1,\ldots,N\}}\{c_{i,\max}\}$, $q = \mathrm{col}(q_1,\ldots,q_N)$, $\xi = \mathrm{col}(\xi_1,\ldots,\xi_N)$, $w = \mathrm{col}(w_1,\ldots,w_N)$, $\widehat{e} = \mathrm{col}(\widehat{e}_1,\ldots,\widehat{e}_N)$, $e = \mathrm{col}(e_1,\ldots,e_{|\mathcal{E}|})$, $x_0 = \mathrm{col}(x_{10},\ldots,x_{N0})$, $h(q,w) = \mathrm{col}(h_1(q_1,w_1),\ldots,h_N(q_N,w_N))$, $H(q,w) = \text{block diag}(H_1(q_1,w_1),\ldots,H_N(q_N,w_N))$, $C(q,\xi,w) = \text{block diag}(C_1(q_1,\xi_1,w_1),\ldots,C_N(q_N,\xi_N,w_N))$, $G(q,w) = \text{block diag}(G_1(q_1,w_1),\ldots,G_N(q_N,w_N))$, $J(q,w) = \text{block diag}(J_1(q_1,w_1),\ldots,J_N(q_N,w_N))$.

Proposition 3.1: Consider N robot manipulators (1) satisfying assumptions **P1** and **P2** where the system parameters are perfectly known. Further assume that the formation graph is infinitesimally and minimally rigid graph $\mathcal{G}$. Then for any end-effector reference configuration x^*, the end-effector formation control problem can be solved by a distributed control law of the following form: for $i = 1,\ldots,N$,

$$u_i = -K_P J_i^T(q_i,a_i)\widehat{e}_i - K_D\xi_i + G_i(q_i,w_i) \tag{16}$$

with gain parameters $K_P, K_D \in \mathbb{R}_{>0}$, where $\widehat{e}_i$, ξ_i are given in (10), (14), respectively.

We note that Proposition 3.1 provides an intermediate solution to Problem 2.1 whose design requires *a priori* precise knowledge of systems' parameters. The result is adapted from [21, Theorem 4.1] for the case without disturbances whose proof can be practically modified and is omitted here. In addition to the established result in [21], we establish below a stronger stability property, namely exponential stability of the closed-loop system using the control law as in Proposition 3.1.

Substituting control law (16) into (1) and using (9), the closed-loop system can compactly be written as

$$\begin{cases} \dot{e} = 2D_z^T\overline{B}^T J(q,a)\xi \\ \dot{\xi} = H^{-1}(q,w)[-K_P J^T(q,a)\widehat{e} - K_D\xi - C(q,\xi,w)\xi] \end{cases} \tag{17}$$

which is a nonautonomous system because the singularity-free $q := q(t)$ is considered here as a time-varying exosignal satisfying $\dot{q} = \xi$, and e is the stacked vector of e_k for all $k \in \{1,\ldots,|\mathcal{E}|\}$ written as $e = \mathrm{col}(\ldots, \|h_i(q_i,w_i) + x_{i0} - h_j(q_j,w_j) - x_{j0}\|^2 - \|z_k^*\|^2, \ldots)$. Now we are ready to show the local exponential convergence to the origin of error distance in edges and joint velocities.

Proposition 3.2: Consider the closed-loop system (17) satisfying all hypotheses in Proposition 3.1. Then there exist positive constants $K_{P,\min}$ and $K_{D,\min}$ such that for all $K_P > K_{P,\min}$ and $K_D > K_{D,\min}$, the equilibrium point $(e,\xi) = (\mathbf{0},\mathbf{0})$ is locally exponentially stable.

The proof of Proposition 3.2 is based on Lyapunov's direct method, and is given in Appendix A.

It is worth noting that the proposed design of distributed control protocols in Proposition 3.1 above is applicable to both displacement-based and distance-based formation control by defining appropriately the potential function of the formation V in (10) and (16). In this paper, we only show the proof for the distance-based case. The proof for the displacement-based case can be obtained following the same procedure and is omitted here.

IV. Main Results

This section is devoted to developing a compete solution to Problem 2.1 following the design methodology introduced in the previous section.

The control law (16) requires complete knowledge on system parameters. Specifically, u_i^v of (15) needs information on parameters for exact gravitational compensation, and u_i^f of (11) needs kinematic parameters in the Jacobian matrix for stabilization control. This knowledge requirement limits the robustness of the resulting closed-loop system. Although robust control of single manipulator's end-effector has been studied in literature (e.g., [23], [24], [25]), imprecision in parameters remains an issue if the task has to be done in a distributed way by a team of manipulators, i.e., central monitoring and control is not allowed.

Correspondingly, we investigate this particular problem in this section, where as before a team of manipulators, whose dynamic and kinematic parameters are not exactly known, has to solve Problem 2.1. Without loss of generality, we can assume that the parameter vector w_i of (1) is written in the form

$$w_i = \bar{w}_i + \Delta w_i \tag{18}$$

where $\bar{w}_i$ represents the nominal part (or approximate value) while Δw_i represents the uncertain part. In this scenario, a direct application of (16) is to use $\bar{w}_i$ instead of w_i, e.g.

$$u_i = -K_P J_i^T(q_i,\bar{a}_i)\widehat{e}_i - K_D\xi_i + G_i(q_i,\bar{w}_i) \tag{19}$$

where

$$\bar{a}_i := a_i(\bar{w}_i)$$

represents the nominal part of $a_i(w_i)$. However, this could lead to the following two immediate consequences. Firstly, the equilibrium point of the closed-loop system (1) and (19) at the origin can be shifted if $G_i(q_i,\bar{w}_i) \neq G_i(q_i,w_i)$ at the desired shape, i.e., e might tend to a non-zero constant vector. Secondly, the mismatch between the nominal Jacobian matrix $J_i(q_i,\bar{a}_i)$ and the actual Jacobian matrix $J_i(q_i,a_i)$ may destabilize the closed-loop system.

To overcome these drawbacks, we will modify (19) such that it can accommodate for parametric uncertainties. Section IV-A presents an additional dynamic compensator for the gravitation compensation. Section IV-B handles the kinematics uncertainties in the Jacobian matrix.

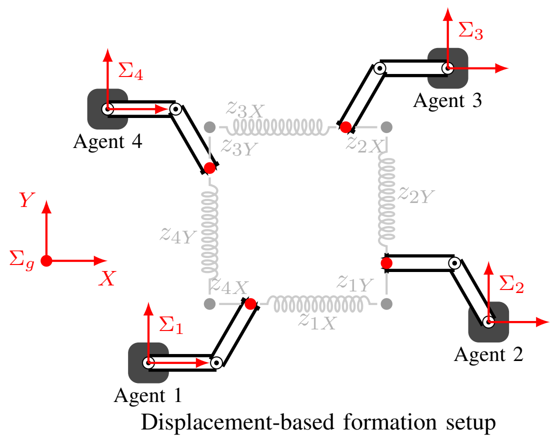

Fig. 2. End-effector formation of 4 two-link planar manipulators in the horizontal plane. Left: displacement-based formation control. Right: distance-based formation control. The springs in gray color are virtual couplings between end-effectors. Σ_1 to Σ_4 in red color are frames attached at manipulator bases.

A. Dynamic compensator design

For a given desired shape, the manipulators have a desired joint-space configuration given by $q^* \in \{q \in \mathbb{R}^{nN} : h(q, w) + x_0 \in \mathcal{S}_W\}$. In the case where $G_i(q_i^*, \bar{w}_i) \neq G_i(q_i^*, w_i)$ and $G_i(q_i^*, w_i) \neq \mathbf{0}$, asymptotic convergence to the desired shape can not be achieved by (19) due to the lack of steady-state error compensation. Hence, an additional compensator is required for asymptotic convergence.

The design of dynamic compensator is based on the internal model principle [26, Chapter 5], which requires the use of integral action to ensure zero steady-state error in the presence of parameter uncertainties. To compensate for the gravitational force, we introduce the following dynamics

$$\dot{\eta}_i = -K_I \eta_i + u_i \tag{20}$$

where K_I is a positive constant. Let η^* be the steady-state of the stacked vector $\eta = \mathrm{col}(\eta_1, \ldots, \eta_N)$. It can be verified that $\eta^* = K_I^{-1} G(q^*, w)$. Let

$$\tilde{\eta} = \eta - \eta^* - H(q, w)\xi. \tag{21}$$

Then using property **P2**, we have the following error dynamics

$$\begin{aligned}\dot{\tilde{\eta}} &= -K_I \eta + u - [C(q, \xi, w) + C^T(q, \xi, w)]\xi \\ &\quad - [u - C(q, \xi, w)\xi - G(q, w)] \\ &= -K_I \tilde{\eta} - K_I H(q, w)\xi - C^T(q, \xi, w)\xi \\ &\quad + G(q, w) - G(q^*, w) \\ &=: -K_I \tilde{\eta} + \psi(t, e, \xi, w)\end{aligned} \tag{22}$$

where

$$\begin{aligned}\psi(t, e, \xi, w) = &-K_I H(q(t), w)\xi - C^T(q(t), \xi, w)\xi \\ &+ G(q(t), w) - G(q^*, w).\end{aligned} \tag{23}$$

Lemma 4.1: Consider error dynamics system in (22). There is a smooth function $V_\eta(\tilde{\eta})$ satisfying

$$\begin{aligned}\underline{\kappa}_0 \|\tilde{\eta}\|^2 \le V_\eta(\tilde{\eta}) \le \bar{\kappa}_0 \|\tilde{\eta}\|^2 \\ \dot{V}_\eta|_{(22)} \le -\kappa_0 \|\tilde{\eta}\|^2 + \varphi_1(\|e\|) + \varphi_2(\|\xi\|)\end{aligned} \tag{24}$$

for all $(\tilde{\eta}, e, \xi) \in \mathbb{R}^{nN} \times \mathbb{R}^{l|\mathcal{E}|} \times \mathbb{R}^{nN}$, where constants $\underline{\kappa}_0, \bar{\kappa}_0, \kappa_0 > 0$ and functions $\varphi_1, \varphi_2 \in \mathcal{K}_\infty$. Moreover, there is a neighborhood of $s = 0$ such that, for all $s : s^2 \le r_1^*$,

$$\varphi_1(s) \le \kappa_1 s^2, \quad \varphi_2(s) \le \kappa_2 s^2$$

for constants $\kappa_1, \kappa_2, r_1^* > 0$.

The proof of Lemma 4.1 is given in Appendix B.

B. Robust stabilization

In the first part of this subsection, we analyze the asymptotic stability of the closed-loop systems when we can only rely on a limited information about the nominal (approximate) Jacobian matrix and the bound of the mismatches with respect to the actual ones. When the bound is sufficiently small, we present a sufficient condition on the control gains that guarantees asymptotic stability. In the second part, we propose an adaptive Jacobian control law that can relax the above mentioned mismatch bound. The adaptive law uses direct cancellation and guarantees asymptotic stability of the closed-loop systems.

1) Approximate Jacobian approach: Let us assume the following property on the Jacobian matrix.

P4 The mismatch between the real Jacobian matrix $J(q, a)$ and the nominal Jacobian matrix $J(q, \bar{a})$ is upper-bounded in the following sense: there is a known positive constant δ such that

$$\|J(q, \Delta a)\| \le \delta, \quad J(q, \Delta a) := J(q, \bar{a}) - J(q, a) \tag{25}$$

holds for all $q \in \mathbb{R}^{nN}$ and all $w \in \mathbb{W}$. In (25), $J(q, \bar{a})$ is nonsingular and upper bounded

$$\|J(q, \bar{a})\| \le c_{\bar{J}}$$

for all $q \in \mathbb{R}^{nN}$, where $c_{\bar{J}}$ is a known positive constant.

Remark 4.1: Condition **P4** describes quantitatively the accuracy of the system parameters, whose value will affect the choice of design parameters in the controller. The matrix $J(q, \bar{a})$ is also known as the approximate Jacobian matrix in manipulator task-space control literature [24].

By adding (20) to (16), we consider the following controller

$$\begin{cases} u_i = -K_P J_i^T(q_i, \bar{a}_i)\hat{e}_i - K_D\xi_i + K_I\eta_i \\ \dot{\eta}_i = -K_I\eta_i + u_i \end{cases} \quad (26)$$

where $\bar{a}$ is the nominal (approximate) value of actual parameters a, and constants K_P, K_D, K_I are positive gains to be designed. By substituting (26) to (1), and using coordinate transformation (9), the error dynamics of (e, ξ) satisfies

$$\begin{cases} \dot{e} = 2D_z^T \overline{B}^T J(q,a)\xi \\ \dot{\xi} = H^{-1}(q,w)[-K_P J^T(q,\bar{a})\hat{e} - K_D\xi + f(t,\tilde{\eta},e,\xi,w)] \end{cases} \quad (27)$$

where $J(q, \bar{a})$ is the nominal (approximate) Jacobian matrix with $\dot{\bar{a}} = \mathbf{0}$, and

$$f(t,\tilde{\eta},e,\xi,w) = K_I\tilde{\eta} + K_I\eta^* + K_I H(q,w)\xi - C(q,\xi,w)\xi - G(q,w). \quad (28)$$

Lemma 4.2: Consider error dynamics system in (27) satisfying **P1** – **P3**. There is a smooth function $U_1(t, e, \xi)$ such that

$$\begin{aligned} &W_1(e,\xi) \le U_1(t,e,\xi) \le W_2(e,\xi) \\ &\dot{U}_1|_{(27)} \le -\alpha\hat{e}^T J(q(t),\bar{a})K_P J^T(q(t),\bar{a})\hat{e} - \xi^T K_D\xi \\ &\quad + \rho(t,e,\xi,\bar{a})\left[J^T(q(t),\bar{a}) - J^T(q(t),a)\right]\hat{e} \\ &\quad + \phi_\alpha(t,\tilde{\eta},e,\xi,w) \end{aligned} \quad (29)$$

for all $t \ge 0$ and all $(\tilde{\eta}, e, \xi) \in \mathbb{R}^{nN} \times \mathbb{R}^{l|\mathcal{E}|} \times \mathbb{R}^{nN}$, where α is a positive constant, $W_1(e,\xi), W_2(e,\xi), \phi_\alpha(t,\tilde{\eta},e,\xi,w)$ are continuous functions, and

$$\rho(t,e,\xi,\bar{a}) = \alpha K_P \hat{e}^T J(q(t),\bar{a}) - K_P\xi^T.$$

Moreover, (29) has the following local version properties:

(i) There are constants $r_2^* > 0$, $\alpha^* > 0$ and $K_P^* > 0$ such that for any $0 < \alpha < \alpha^*$, $K_D > 0$ and $K_P > K_P^*$, $U_1(t, e, \xi)$ is locally positive definite. In other words, there are constants $\underline{k}_1, \underline{k}_2, \bar{k}_1, \bar{k}_2 > 0$ such that $\forall t \ge 0$, $\forall e : \|e\|^2 \le r_2^*$, $\forall \xi : \|\xi\|^2 \le r_2^*$.

$$\begin{aligned} W_1(e,\xi) &= \underline{k}_1\|e\|^2 + \underline{k}_2\|\xi\|^2 \\ W_2(e,\xi) &= \bar{k}_1\|e\|^2 + \bar{k}_2\|\xi\|^2. \end{aligned}$$

Given α and K_I, there are constants $k_0, k_1, k_2 > 0$ such that the function $\phi_\alpha(t, \tilde{\eta}, e, \xi, w)$ satisfies

$$\begin{aligned} &\phi_\alpha(t,\tilde{\eta},e,\xi,w) \le k_0\|\tilde{\eta}\|^2 + k_1\|e\|^2 + k_2\|\xi\|^2 \quad (30) \\ &\forall t \ge 0, \|e\|^2 \le r_2^*, \|\xi\|^2 \le r_2^*, \tilde{\eta} \in \mathbb{R}^{nN}, w \in \mathbb{W}. \end{aligned}$$

(ii) If $J(q(0), \bar{a})$ is nonsingular, there is a constant $r_{\bar{J}}^*$ such that $J(q,\bar{a})J^T(q,\bar{a})$ is full rank for all q in the compact set

$$Q_{r_{\bar{J}}^*} := \{q : \|q - q(0)\|^2 \le r_{\bar{J}}^*\}.$$

(iii) The matrix $D_z^T \overline{B^T B} D_z$ can be expressed as a smooth function of e, i.e., there is a smooth matrix-valued function $Q(e)$ such that $D_z^T \overline{B^T B} D_z = Q(e)$ [27], [6]. If the formation graph $\mathcal{G}$ is infinitesimally and minimally rigid, there is a constant r_z^* such that $D_z^T \overline{B^T B} D_z$ is full rank in the compact set

$$Q_{r_z^*} := \{e : \|e\|^2 \le r_z^*\}.$$

From Lemma 4.2, whose proof is given in Appendix B, we have the following two remarks. Firstly, it is difficult to make the time derivative of U_1 globally negative definite, because of the possible singularities in both manipulator Jacobian matrix $J(q, \bar{a})$ and the rigidity matrix $D_z^T \overline{B^T B} D_z$. Correspondingly, we will present local stability analysis instead. Secondly, when the manipulator Jacobian matrix is exactly known, i.e., $J(q, \bar{a}) = J(q, a)$, the second line of $\dot{U}_1|_{(27)}$ in (29) is zero. As a result, Lemma 4.2 reduces to an intermediate result for proving Proposition 3.2.

With the aforementioned preparation, we are ready for the following proposition.

Proposition 4.1: Consider the closed-loop system given by (22) and (27) with small δ in (25). Then for any given $K_I > 0$ there exist $K_{P,\min} > 0$ and $\beta_{\min}$ such that the system consisting of (22) and (27) is locally exponentially stable at $(\tilde{\eta}, e, \xi) = (\mathbf{0}, \mathbf{0}, \mathbf{0})$ with $K_P > K_{P,\min}$ and $K_D/K_P > \beta_{\min}$.

Proof of Proposition 4.1: Consider the closed-loop system composed of (22) and (27). Define a time-varying Lyapunov function candidate $U_2(t, \tilde{\eta}, e, \xi)$ by

$$U_2(t,\tilde{\eta},e,\xi) = \varepsilon^{-1}V_\eta(\tilde{\eta}) + U_1(t,e,\xi) \quad (31)$$

where $V_\eta(\tilde{\eta})$ and $U_1(t, e, \xi)$ are given in (24) and (29), respectively, for a sufficiently small constant $\varepsilon > 0$ to be determined later below (c.f. (35)). It is obvious that U_2 is locally positive definite (uniformly on t).

Next, we are going to show that the time derivative of (31) can be made locally negative definite uniformly with respect to all $t \ge 0$. To this end, recall Lemma 4.1 and Lemma 4.2, and choose $r^* > 0$ such that $r^* \le \min\{r_1^*, r_2^*, r_z^*\}$. Define a compact set $\mathcal{Q}_{r^*}$ by

$$\mathcal{Q}_{r^*} := \{e : \|e\|^2 \le r^*\}. \quad (32)$$

Define a set $\mathbb{Q}_\epsilon$ away from kinematic singularities by

$$\mathbb{Q}_\epsilon := \{q : \mathrm{dist}(q, \mathrm{Q}) \ge \epsilon\} \quad (33)$$

for some small positive constant ϵ, where Q is the set of manipulators kinematic singularities, and $Q_{r_{\bar{J}}^*} \subset \mathbb{Q}_\epsilon$. It has been shown in Lemma 4.2 that $D_z^T \overline{B^T B} D_z$ can be a smooth function of e. Therefore, we define positive constants λ_e and $\lambda_{\bar{J}}$ by

$$\begin{aligned} \lambda_e &= \max_{e \in \mathcal{Q}_{r^*}} \lambda_{\max}\{D_z^T \overline{B^T B} D_z\} \\ \lambda_{\bar{J}} &= \min_{e \in \mathcal{Q}_{r^*}, q \in \mathbb{Q}_\epsilon} \lambda_{\min}\{D_z^T \overline{B}^T J(q,\bar{a})J^T(q,\bar{a})\overline{B}D_z\}. \end{aligned} \quad (34)$$

For the time derivative (29), by using $\hat{e} = 2\overline{B}D_z e$, condition **P4**, and the Young's inequality, we have

$$\begin{aligned} &\rho(t,e,\xi,\bar{a})\left[J^T(q,\bar{a}) - J^T(q,a)\right]\hat{e} \\ &= \left[\alpha K_P\hat{e}^T J(q,\bar{a}) - K_P\xi^T\right]\left[J^T(q,\bar{a}) - J^T(q,a)\right]\hat{e} \\ &= \alpha K_P\hat{e}^T J(q,\bar{a})J^T(q,\tilde{a})\hat{e} - K_P\xi^T J^T(q,\tilde{a})\hat{e} \\ &\le 4\alpha K_P \underbrace{\|J(q,\bar{a})\|}_{\le c_{\bar{J}}} \underbrace{\|J(q,\tilde{a})\|}_{\le\delta} \|\overline{B}D_z e\|^2 \\ &\quad + 2K_P \underbrace{\|J(q,\tilde{a})\|}_{\le\delta} \|\overline{B}D_z e\|\|\xi\| \\ &\le 4\alpha K_P c_{\bar{J}}\delta\lambda_e\|e\|^2 + K_P\delta(\lambda_e\|e\|^2 + \|\xi\|^2). \end{aligned}$$

Then the time derivative of $U_2(t,\tilde{\eta},e,\xi)$ along the trajectory of (22) and (27) satisfies

$$\begin{aligned}\dot{U}_2|_{(22)+(27)} &= \varepsilon^{-1}\dot{V}_\eta(\tilde{\eta})|_{(22)} + \dot{U}_1(t,e,\xi)|_{(27)} \\ &\leq \varepsilon^{-1}(-\kappa_0\|\tilde{\eta}\|^2 + \kappa_1\|e\|^2 + \kappa_2\|\xi\|^2) \\ &\quad - \alpha K_P \lambda_{\bar{J}}\|e\|^2 - K_D\|\xi\|^2 \\ &\quad + 4\alpha K_P c_{\bar{J}}\delta\lambda_e\|e\|^2 + K_P\delta(\lambda_e\|e\|^2 + \|\xi\|^2) \\ &\quad + k_0\|\tilde{\eta}\|^2 + k_1\|e\|^2 + k_2\|\xi\|^2 \\ &\leq -\big(\varepsilon^{-1}\kappa_0 - k_0\big)\|\tilde{\eta}\|^2 - \big(\alpha K_P\lambda_{\bar{J}} - \varepsilon^{-1}\kappa_1 \\ &\quad - 4\alpha K_P c_{\bar{J}}\delta - K_P\delta\lambda_e - k_1\big)\|e\|^2 \\ &\quad - \big(K_D - \varepsilon^{-1}\kappa_2 - K_P\delta - k_2\big)\|\xi\|^2\end{aligned}$$

for all $t \geq 0$, and all $\tilde{\eta} \in \mathbb{R}^{nN}, e : \|e\|^2 \leq r^*, \xi : \|\xi\|^2 \leq r^*$.

The above time derivative can be made negative definite by the following steps:

1) Fix constant α such that $0 < \alpha < c_{\min}/c_{\max}$.
2) Choose constant $K_I > 0$.
3) Compute constants $\kappa_0, \kappa_1, \kappa_2$ in Lemma 4.1 for the given K_I and r_1^*. Compute constants k_0, k_1, k_2 in Lemma 4.2 for the given α, K_I and r_2^*. Compute constant $\lambda_{\bar{J}}$ and $c_{\bar{J}}$.
4) Fix constant ε such that
$$\varepsilon^{-1}\kappa_0 - k_0 > 1. \tag{35}$$
5) Let $\delta^* = \frac{\alpha\lambda_{\bar{J}}}{4\alpha c_{\bar{J}} + \lambda_e}$.
   - If $\delta < \delta^*$, then choose constant $K_P > 0$ such that
   $$K_P[\alpha\lambda_{\bar{J}} - (4\alpha c_{\bar{J}} + \lambda_e)\delta] - \varepsilon^{-1}\kappa_1 - k_1 > 1.$$
   Choose constant $K_D > 0$ such that
   $$K_D - \varepsilon^{-1}\kappa_2 - K_P\delta - k_2 > 1.$$
   - If $\delta \geq \delta^*$, then we can not find $K_P, K_D > 0$ such that the time derivative is negative.

Hence, if δ is small enough, there are constants $K_P, K_I, K_D > 0$ such that

$$\dot{U}_2|_{(22)+(27)} \leq -\|\tilde{\eta}\|^2 - \|e\|^2 - \|\xi\|^2. \tag{36}$$

Note that the previous analysis are on the time-varying Lyapunov function U_2 that depends on the compensation error $\tilde{\eta}$, the joint's velocities ξ, and the *distortion* of the shape measured by the error signal e. In the sequel, we will show that the final positions of the end-effectors converge to $\mathcal{S}_W$.

Recall Lemma 4.1, Lemma 4.2, and Lyapunov function (31). Let us define the following sets

$$\Omega_r^1 := \{(\tilde{\eta},e,\xi) : \varepsilon^{-1}\underline{\kappa}_0\|\tilde{\eta}\|^2 + \underline{k}_1\|e\|^2 + \underline{k}_2\|\xi\|^2 \leq r\}$$
$$\Omega_r^2 := \{(\tilde{\eta},e,\xi) : \varepsilon^{-1}\bar{\kappa}_0\|\tilde{\eta}\|^2 + \bar{k}_1\|e\|^2 + \bar{k}_2\|\xi\|^2 \leq r\}$$

and define a time-dependent set

$$\mathcal{S}_{W_{r,t}} := \{(\tilde{\eta},e,\xi) : U_2(t,\tilde{\eta},e,\xi) \leq r\} \tag{37}$$

for constant $r > 0$. It can be verified that $\Omega_r^2 \subset \mathcal{S}_{W_{r,t}} \subset \Omega_r^1$ for all $t \geq 0$, and r can be chosen such that $\Omega_r^1 \subset \{(\tilde{\eta},e,\xi) : \tilde{\eta} \in \mathbb{R}^{nN}, \|e\|^2 \leq r^*, \|\xi\|^2 \leq r^*\}$.

Since $\dot{U}_2|_{(22)+(27)} \leq 0$, we have $U_2(t,\tilde{\eta}(t),e(t),\xi(t)) \leq U_2(0,\tilde{\eta}(0),e(0),\xi(0))$ for all $t \geq 0$. It follows that any solution starting at $(0,\tilde{\eta}(0),e(0),\xi(0))$ stays in $\mathcal{S}_{W_{r,t}}$, and consequently in Ω_r^1 for all $t \geq 0$. Hence, the solution is bounded for all t. Moreover, by using [28, Theorem 4.10], the origin defined by signals $(\tilde{\eta},e,\xi)$ is exponentially stable. Then, we have that the joint's velocities $\xi(t) \to 0$ exponentially fast as $t \to \infty$; therefore, the total distance travelled by the end-effectors is bounded. Hence, if $q(0) \in \mathbb{Q}_\epsilon$ with sufficiently large ϵ, $x(t) \to \mathcal{S}_W$ as $t \to \infty$ with $q(t)$ be always from the kinematics singularities. Q.E.D.

Remark 4.2: From the proof of Proposition 4.1, we notice that the set $\mathcal{S}_{W_{r,t}}$ in (37) describes how "close" (quantified by r) the manipulators are to the desired shape, and the set $\mathbb{Q}_\epsilon$ in (33) describes how "far" (quantified by ϵ) the manipulators are from the kinematic singularities. The former directly implies that our result is only valid in a local sense. The latter is a common condition for manipulators to operate away from singular configurations. Note that even for two configurations with the same r, their ϵ can be different. An illustrative example is shown in Fig. 1. In this example, since all the manipulators move in the horizontal plane, subsystem η for gravitational compensation can be removed. In Fig. 1, the dotted squares in different colors represent some possible reachable desired formation. When manipulators arrive and stop at any of these squares (e.g., squares red and light green), $(e,\xi) = (\mathbf{0},\mathbf{0})$. Hence, we can choose $r = 0$ in $\mathcal{S}_{W_{r,t}}$ for them; however, the former admits a smaller ϵ than the latter. This is because the red square is closer to singular configurations, where the Jacobian is not full rank as opposed to that of the green one.

2) Adaptive Jacobian approach: As mentioned before, the control law (26) requires that the mismatch between actual Jacobian and nominal Jacobian is bounded and sufficiently small for guaranteeing the locally exponentially stability. In order to relax this, we present an adaptive Jacobian approach in the following theorem.

Specifically, instead of using the nominal Jacobian matrix $J(q,\bar{a})$ in (26), we propose a new controller by using adaptive Jacobian matrix $J(q,\hat{a})$ based on the linear parameterization property **P2**. The parameter estimate law for estimating a is designed as follows:

$$\dot{\hat{a}}_i = -Z_i^T(q_i,\hat{e}_i)\big[\alpha Z_i(q_i,\hat{e}_i)\hat{a}_i - \xi_i\big] \tag{38}$$

where constant $\alpha > 0$ is a design parameter, and function Z_i is the kinematic regressor matrix given in **P3**. Let $\tilde{a}_i$ be the parameter estimation error defined by

$$\tilde{a}_i = \hat{a}_i - a_i, \quad i = 1,\dots,N.$$

For the sake of presentation convenience, we denote $\hat{a} = \mathrm{col}(\hat{a}_1,\dots,\hat{a}_N)$, $\tilde{a} = \mathrm{col}(\tilde{a}_1,\dots,\tilde{a}_N)$, and $Z(q,\hat{e}) = \text{block diag}(Z_1(q_1,\hat{e}_1),\dots,Z_N(q_N,\hat{e}_N))$.

Then, based on (22) and (27), when $J(q,\bar{a})$ in (27) is further substituted by $J(q,\hat{a})$ with $\hat{a}$ satisfying (38), we can write down the following closed-loop error dynamics

$$\begin{cases}\dot{\hat{a}} = -Z^T(q,\hat{e})\big[\alpha Z(q,\hat{e})\hat{a} - \xi\big] \\ \dot{\tilde{\eta}} = -K_I\tilde{\eta} + \psi(t,e,\xi,w) \\ \dot{e} = 2D_z^T\overline{B}^T J(q,a)\xi \\ \dot{\xi} = H^{-1}(q,w)[-K_P J^T(q,\hat{a})\hat{e} - K_D\xi \\ \qquad + f(t,\tilde{\eta},e,\xi,w)]\end{cases} \tag{39}$$

where functions ψ and f are given in (23) and (28), respectively.

Now we are ready to give the main result of this study.

Theorem 4.1: Consider N uncertain robot manipulators (1) satisfying assumptions **P1**, **P2** and **P3**. Assume that the formation graph $\mathcal{G}$ is infinitesimally and minimally rigid, and $\mathbf{Q}_{w_i}$ is nonempty for all w_i in a compact set. Then for any end-effector reference configuration x^*, there exist positive constants K_P, K_D, K_I and α, such that the end-effector formation control problem can be solved by the following distributed control law, for $i = 1, \dots, N$,

$$\begin{cases} u_i = -K_P J_i^T(q_i, \hat{a}_i)\widehat{e}_i - K_D \xi_i + K_I \eta_i \\ \dot{\hat{a}}_i = -Z_i^T(q_i, \widehat{e}_i)\big[\alpha Z_i(q_i, \widehat{e}_i)\hat{a}_i - \xi_i\big] \\ \dot{\eta}_i = -K_I \eta_i + u_i \end{cases} \tag{40}$$

where $\widehat{e}_i$, ξ_i are given in (10), (14), respectively.

In particular, there are constants $\alpha^*, K_{P,\min}, K_{D,\min} > 0$ for the closed-loop error dynamics (39) such that if $0 < \alpha < \alpha^*$, $K_P > K_{P,\min}$, $K_D > K_{D,\min}$, $K_I > 0$ then the closed-loop system (39) is Lyapunov stable and the state $(\tilde{\eta}, e, \xi)$ converges to zero asymptotically.

Proof of Theorem 4.1: Consider the closed-loop system (39). Let us begin with defining a Lyapunov function $U_3(t, \tilde{a}, \tilde{\eta}, e, \xi)$ by

$$U_3(t, \tilde{a}, \tilde{\eta}, e, \xi) = \frac{1}{2}\tilde{a}^T K_P \tilde{a} + \varepsilon^{-1} V_\eta(\tilde{\eta}) + U_1(t, e, \xi) \tag{41}$$

where $V_\eta(\tilde{\eta})$ and $U_1(t, e, \xi)$ are given in (24) and (29), respectively, for a sufficiently small constant $\varepsilon > 0$ to be determined later below. By Lemma 4.2, it can be easily verified that $U_3(t, \tilde{a}, \tilde{\eta}, e, \xi)$ is locally positive definite.

Next, before carrying out the Lyapunov analysis, we show the following parameter linearization condition:

- Since the manipulator Jacobian matrix satisfies linear parameterized condition **P3**, $\alpha \widehat{e}^T J(q, \tilde{a}) K_P J^T(q, \hat{a})\widehat{e}$ can be rewritten as

$$\begin{aligned} \alpha \widehat{e}^T J(q, \tilde{a}) K_P J^T(q, \hat{a})\widehat{e} &= \alpha K_P [J^T(q, \tilde{a})\widehat{e}]^T J^T(q, \hat{a})\widehat{e} \\ &= \alpha K_P [Z(q, \widehat{e})\tilde{a}]^T Z(q, \widehat{e})\hat{a} \\ &= \alpha K_P \tilde{a}^T Z^T(q, \widehat{e}) Z(q, \widehat{e})\hat{a}. \end{aligned} \tag{42}$$

- Using **P3** again, $-K_P \widehat{e}^T J(q, \tilde{a})\xi$ can be rewritten as

$$\begin{aligned} -K_P \widehat{e}^T J(q, \tilde{a})\xi &= -K_P [J^T(q, \tilde{a})\widehat{e}]^T \xi \\ &= -K_P [Z(q, \widehat{e})\tilde{a}]^T \xi \\ &= -K_P \tilde{a}^T Z^T(q, \widehat{e})\xi. \end{aligned} \tag{43}$$

Then the time derivative of U_3 along the trajectory of the closed-loop system (39) satisfies

$$\begin{aligned} \dot{U}_3|_{(39)} = &-K_P \tilde{a}^T Z^T(q, \widehat{e})\big[\alpha Z(q, \widehat{e})\hat{a} - \xi\big] \\ &+ \varepsilon^{-1}\dot{V}_\eta|_{(39)} + \dot{U}_1|_{(39)}. \end{aligned}$$

Then by using (24) and (29), we obtain

$$\begin{aligned} \dot{U}_3|_{(39)} \le &-\varepsilon^{-1}(\kappa_0\|\tilde{\eta}\|^2 + \varphi_1(\|e\|) + \varphi_2(\|\xi\|)) \\ &- \alpha \widehat{e}^T J(q, \hat{a}) K_P J^T(q, \hat{a})\widehat{e} - \xi^T K_D \xi \\ &+ \phi_\alpha(t, \tilde{\eta}, e, \xi, w) \end{aligned} \tag{44}$$

for all $t \ge 0$ and all $(\tilde{a}, \tilde{\eta}, e, \xi) \in \mathbb{R}^{np} \times \mathbb{R}^{nN} \times \mathbb{R}^{l|\mathcal{E}|} \times \mathbb{R}^{nN}$, where functions φ_1, φ_2 and constant κ_0 are the same as those in Lemma 4.1, and function ϕ_α is the same as that in Lemma 4.2.

Recall the set $\mathcal{Q}_{r^*}$ and $\mathbb{Q}_\epsilon$ defined in (32) and (33), respectively. Let $\mathbb{A}$ be a compact set containing a such that $J(q, \hat{a})$ is full rank for all $a \in \mathbb{A}$ and all $q \in \mathbb{Q}_\epsilon$. Let

$$\lambda_{\hat{J}} = \min_{e \in \mathcal{Q}_{r^*}, q \in \mathbb{Q}_\epsilon, \hat{a} \in \mathbb{A}} \lambda_{\min}\{D_z^T \overline{B}^T J(q, \hat{a}) J^T(q, \hat{a}) \overline{B} D_z\}. \tag{45}$$

Then, by applying Lemma 4.1 and Lemma 4.2 to (44), it is not difficult to derive the following expression

$$\begin{aligned} \dot{U}_3|_{(39)} \le &-(\varepsilon^{-1}\kappa_0 - k_0)\|\tilde{\eta}\|^2 - (\alpha\lambda_{\hat{J}} K_P - \varepsilon^{-1}\kappa_1 - k_1)\|e\|^2 \\ &- (K_D - \varepsilon^{-1}\kappa_2 - k_2)\|\xi\|^2 \end{aligned}$$

for all $t \ge 0$ and all $\tilde{a} \in \mathbb{R}^{np}, \tilde{\eta} \in \mathbb{R}^{nN}, e : \|e\|^2 \le r^*, \xi : \|\xi\|^2 \le r^*$.

Similar to the analysis in the proof of Proposition 4.1, we can first fix parameter ε such that $\varepsilon^{-1}\kappa_0 - k_0 > 0$. Subsequently, we can choose K_D and K_D such that

$$\alpha\lambda_{\hat{J}} K_P - \varepsilon^{-1}\kappa_1 - k_1 > 1, \quad K_D - \varepsilon^{-1}\kappa_2 - k_2 > 1. \tag{46}$$

Hence, we obtain

$$\dot{U}_3|_{(39)} \le -\|\tilde{\eta}\|^2 - \|e\|^2 - \|\xi\|^2$$

which implies that U_3 is non-increasing. Since U_3 is locally positive definite, the states $(\tilde{\eta}, e, \xi, \tilde{a})$ of system (39) starting from a small neighborhood of origin are all bounded over time interval $[0, \infty)$. Hence, by continuity, $\ddot{U}_3$ along the trajectory of closed-loop system is also bounded. Using Barbalat's Lemma [13, pp. 123], it implies $\tilde{\eta}$, e and ξ converges to zero. Similarly as in Proposition 3.1, we can conclude that $x(t) \to \mathcal{S}_W$ as $t \to \infty$ with manipulators operating away from kinematic singularities. The proof is complete. Q.E.D.

Remark 4.3: Assume that the system parameters $w = \mathrm{col}(w_1, \cdots, w_N)$ are unknown, but belong to a known compact set $\mathbb{W}$, and the manipulators start away from kinematic singularities. Fix sets $\mathcal{Q}_{r^*}$ and $\mathbb{Q}_\epsilon$ defined in (32) and (33) on the basis of initial joint positions and formation errors, respectively. Fix set $\mathbb{A}$ such that it contains a and $J(q, \hat{a})$ is full rank for all $\hat{a} \in \mathbb{A}$ and $q \in \mathbb{Q}_\epsilon$. Then the following steps towards controller (40) can be taken.

1) Choose constant α such that

$$0 < \alpha < \alpha^* \quad \text{with} \quad \alpha^* = c_{\min}/c_{\max}.$$

2) Choose constant $K_I > 0$.
3) Compute constants $\kappa_0, \kappa_1, \kappa_2$ in Lemma 4.1 for the given K_I and $r_1^* = r^*$. Compute constants k_0, k_1, k_2 in Lemma 4.2 for the given α, K_I and $r_2^* = r^*$. Compute constant $\lambda_{\hat{J}}$ defined in (45).
4) Fix constant ε such that $\varepsilon^{-1}\kappa_0 - k_0 > 0$.
5) Choose constant K_D such that

$$K_D > K_{D,\min} \quad \text{with} \quad K_{D,\min} = \varepsilon^{-1}\kappa_2 + k_2 + 1.$$

6) Choose constant K_P such that

$$K_P > K_{P,\min} \text{ with } K_{P,\min} = \max\left\{\frac{\varepsilon^{-1}\kappa_1 + k_1 + 1}{\alpha\lambda_{\hat{J}}}, K_P^*\right\}$$

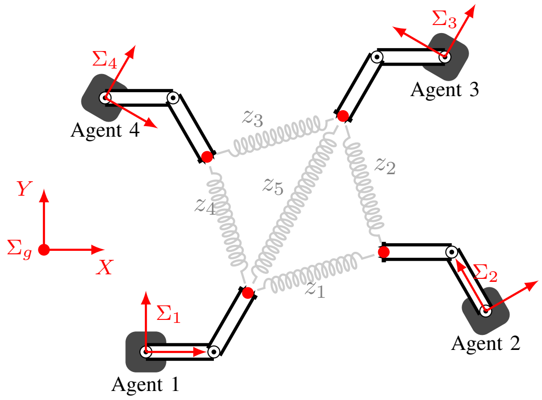

Fig. 3. Distanced-based end-effector formation of 4 two-link planar manipulators. Σ_g is the global frame. Σ_1 to Σ_4 are local frames fixed to the base of each manipulator. These local coordinate systems do not need to have a common sense of orientation,

with K_P^* as given in Lemma 4.2.

In the above, the third step amounts to computing the constant gains related to unknown functions in compact sets. These constants can be approximated numerically by computing a grid of points sufficiently dense and properly distributed in compact sets.

Remark 4.4: Let $p(t)$ be the geometric centroid of the formation by $p(t) = \frac{1}{N}\sum_{i=1}^{N} x_i(t)$. Unlike the point mass model case [4], this centroid is not necessarily stationary under the proposed control law even when the manipulator parameters are all perfectly known.

Remark 4.5: The internal model η_i of (40) is essentially an integrator [26, Chapter 12.3]. This property can be shown by a direct coordinate transformation. By substituting u_i of (40) into subsystem η_i, direct calculation gives

$$\begin{aligned}\dot{\eta}_i &= -K_I\eta_i + [-K_P J_i^T(q_i,\bar{a}_i)\widehat{e}_i - K_D\xi_i + K_I\eta_i] \\ &= -K_P J_i^T(q_i,\bar{a}_i)\widehat{e}_i - K_D\xi_i.\end{aligned}$$

Define an output vector y_i by

$$y = \Lambda J_i^T(q_i,\bar{a}_i)\widehat{e}_i + \xi_i$$

where $\Lambda = K_D^{-1}K_P$. Then the input u_i of (40) can be rewritten as

$$u_i = -K_P J_i^T(q_i,\bar{a}_i)\widehat{e}_i - K_D\xi_i - \bar{K}_I\int_0^t y(s)ds$$

where $\bar{K}_I = K_I K_D$, *cf.* the PID form in [23], [24].

V. Further Discussion

The proposed gradient-based designs in aforementioned sections are applicable to both displacement- and distance-based formation control. For the displacement-based formation control, the proof can be carefully modified by replacing $2\overline{B}D_z$ with $\overline{B}$ in the closed-loop system and relevant Lyapunov analysis due to (12) and (13).

For the distance-based formation control, just like the gradient-based design for the kinematic point case [4], the manipulators can maintain their own coordinate system without the use of common frame of reference. In other words, the proposed distributed gradient control law can be implemented using its local frame of reference and using only local relative measurement systems, both of which are desirable in practice.

The realization using only local frame of reference can be shown by a suitable coordinate transformation. As depicted in Fig. 3, let Σ_i denote the local frame fixed to the base of the ith manipulator. By adopting a group of new notation in which superscripts are used to denote local coordinate system, the manipulator dynamics and kinematics can be written as

$$\begin{aligned}H_i(q_i,w_i)\ddot{q}_i + C_i(q_i,\dot{q}_i,w_i)\dot{q}_i + G_i^i(q_i,w_i) &= u_i^i \\ x_i^i &= h_i^i(q_i,w_i)\end{aligned}$$

where $i \in \{1,\ldots,N\}$, x_i^i, u_i^i, $h_i^i(q_i,w_i)$ and $G_i^i(q_i,w_i)$ are the end-effector position, the control input, the forward kinematics and the gravitational torque, respectively, that defined with respect to Σ_i. The states $q_i, \dot{q}_i, \ddot{q}_i \in \mathbb{R}^n$ and functions $H_i(q_i,w_i)$, $C_i(q_i,\dot{q}_i,w_i)$ are the same as that in previous sections, because joint angle, the kinetic energy and the forward kinematic with respect to base frame are not defined with respect to the world frame Σ_g.

Let x_i^g and x_{i0} be the end-effector position and base position of i-th manipulator, respectively, with respect to the global frame Σ_g. Then we have

$$x_i^g = R_i^g x_i^i + x_{i0} \tag{47}$$

where $R_i^g \in \mathrm{SO}(m)$ is a rotation matrix defining the rotation transformation from Σ_i to Σ_g. Taking the time derivative of (47) gives us

$$J_i^g(q_i,a_i)\dot{q}_i = R_i^g J_i^i(q_i,a_i)\dot{q}_i. \tag{48}$$

where $J_i^i(q_i,a_i) = \frac{\partial h_i^i(q_i,w_i)}{\partial q_i}$. Suppose that all the manipulators sense relative end-effector positions of their neighbors with respect to their own base frame Σ_i

$$z_{ij}^i = z_k^i = x_i^i - x_j^i, \quad j \in \mathcal{N}_i$$

where x_j^i is the jth manipulator's end-effector position with respect to Σ_i. Thus the error signal for the edge k is $e_{ij}^i = e_k^i = \|z_k^i\|^2 - \|z_k^*\|^2$ satisfying $e_{ij}^i = e_{ij}$, where e_{ij} is the error signal with respect to Σ_g. From (10), it can be expressed locally as

$$\widehat{e}_i^i = \sum_{j\in\mathcal{N}_i} b_{ik}e_k^i(x_i^i - x_j^i) = \sum_{j\in\mathcal{N}_i} e_{ij}^i(x_i^i - x_j^i).$$

satisfying

$$\widehat{e}_i = \sum_{j\in\mathcal{N}_i} e_{ij}^i(x_i - x_j) = \sum_{j\in\mathcal{N}_i} e_{ij}^i R_i^g(x_i^i - x_j^i) = R_i^g\widehat{e}_i^i. \tag{49}$$

Hence, the gradient-based control law for agent i can be designed as

$$\begin{aligned}u_i^i &= -K_P[\underbrace{J_i^i(q_i,\bar{a}_i)}_{\text{using (48)}}]^T\widehat{e}_i^i - K_D\xi_i + K_I\eta_i \\ &= -K_P\underbrace{[(R_i^g)^{-1}J_i^g(q_i,\bar{a}_i)]^T}_{\text{using } R_i^g\in\mathrm{SO}(m)}\widehat{e}_i^i - K_D\xi_i + K_I\eta_i \\ &= -K_P[J_i^i(q_i,\bar{a}_i)]^T\underbrace{R_i^g\widehat{e}_i^i}_{\text{using (49)}} - K_D\xi_i + K_I\eta_i \\ &= -K_P[J_i^g(q_i,\bar{a}_i)]^T\widehat{e}_i - K_D\xi_i + K_I\eta_i = u_i\end{aligned}$$

where u_i is the input specified with respect to Σ_g.

VI. Simulation

In this section, we illustrate the adaptive Jacobian approach based controller presented in Theorem 4.1 with two different numerical simulations. One is a basic example where 4 planar manipulators moving in the horizontal X-Y plane, i.e., $G_i(q_i, w_i) \equiv 0$, $i = 1, \ldots, 4$. In this special case, we demonstrate that the internal model subsystem η_i is not needed any longer to compensate the gravity. The other is a group of general seven degree-of-freedom humanoid manipulator arms working in 3D space are presented to illustrate the effectiveness of the adaptive Jacobian approach.

A. End-effectors formation in 2D

For the simulation setup, we first consider a network of $N = 4$ two-link planar manipulator in the horizontal X-Y plane. For the dynamic model of two-link robot manipulator as in (1), we refer to [13, Example 6.2] and the corresponding nominal values of the parameters are given in Table I for each link. The kinematic model of each two-link robot manipulator is given by

$$x_i = \begin{bmatrix} l_1\cos(q_{i1}) + l_2\cos(q_{i1}+q_{i2}) \\ l_1\sin(q_{i1}) + l_2\sin(q_{i1}+q_{i2}) \end{bmatrix} + x_{i0}$$

and correspondingly, the manipulator Jacobian matrix is

$$J_i(q_i, a_i) = \begin{bmatrix} -l_1\sin(q_{i1}) - l_2\sin(q_{i1}+q_{i2}) & -l_2\sin(q_{i1}+q_{i2}) \\ l_1\cos(q_{i1}) + l_2\cos(q_{i1}+q_{i2}) & l_2\cos(q_{i1}+q_{i2}) \end{bmatrix}$$

for $i = 1, 2, 3, 4$, where $q_i = \begin{bmatrix} q_{i1} & q_{i2} \end{bmatrix}^T$, $a_i = \begin{bmatrix} l_1 & l_2 \end{bmatrix}^T$. Then the kinematic singular configurations set is

$$\{q_i \in \mathbb{R}^2 : q_{i1} \in \mathbb{R}, q_{i2} = 0, \pm\pi, \pm 2\pi, \ldots\},\ i = 1, 2, 3, 4.$$

We consider the formation shape of a square with side length of 2 m and the associated formation graph is represented by its incidence matrix given by

$$B = \begin{bmatrix} 1 & 0 & 0 & -1 & 1 \\ -1 & 1 & 0 & 0 & 0 \\ 0 & -1 & 1 & 0 & -1 \\ 0 & 0 & -1 & 1 & 0 \end{bmatrix}$$

and illustrated in Fig. 2 (right). For the numerical simulation setup, the bases of the 4 manipulators are located at $(0, 0)$, $(6, 0)$, $(6, 6)$ and $(0, 6)$, respectively, and the initial joint positions are set to $q_1(0) = [0 \ \ \pi/3]^T$, $q_2(0) = [\pi/2 \ \ \pi/3]^T$, $q_3(0) = [\pi \ \ \pi/3]^T$, $q_4(0) = [3\pi/2 \ \ \pi/3]^T$. All the initial joint velocities are set to zero. The initial values of kinematic parameter estimates are determined as $\hat{a}_i(0) = \begin{bmatrix} 2 & 2 \end{bmatrix}^T$, $i = 1, 2, 3, 4$.

Applying Theorem 4.1, the controller can be specified as

$$\begin{cases} u_i = -K_P J_i^T(q_i, \hat{a}_i)\widehat{e}_i - K_D \xi_i \\ \dot{\hat{a}}_i = -Z_i^T(q_i, \widehat{e}_i)\big[\alpha Z_i(q_i, \widehat{e}_i)\hat{a}_i - \xi_i\big] \end{cases} \tag{50}$$

since all manipulators are considered to operate in the horizontal plane ($G_i(q_i, w_i) \equiv 0$, $i = 1, 2, 3, 4$), the internal model subsystem η_i to compensate the gravity is not needed.

TABLE I
Physical parameters of the two-link planar manipulators.

Symbol	Meaning	Nominal value	
		$i = 1$	$i = 2$
m_i (Kg)	mass of the ith link	1.2	1.0
I_{ci} (Kg·m^2)	ith moment of inertia	0.2250	0.1875
l_i (m)	length of the ith link	1.5	1.5
l_{ci} (m)	distance from the center of the mass of the ith link to the ith joint	0.75	0.75

In order to determine the design parameters K_P, K_D and α, we follow the procedure in Remark 4.3 and choose $r^* = 16^2, \epsilon = \frac{1}{6}\pi$ for the sets $\mathcal{Q}_{r^*}, \mathbb{Q}_\epsilon$. The $\mathbb{A}$ is chosen to be a subset of $\mathbb{R}^8$ whose elements range between 2.0 ± 0.5, i.e., $\hat{a}_{ij}$ satisfies $1.5 \leq \hat{a}_{ij} \leq 2.5$, $i = 1, 2, 3, 4$, $j = 1, 2$. The bounds in **P1** are $c_{i,\min} = 0.16$, $c_{i,\max} = 7.8$, $i = 1, 2, 3, 4$. It follows that we can choose $\alpha = 0.02$. Since there is no η_i-subsystem, we have $K_I = 0$, $\kappa_0 = 0$, $\kappa_1 = 0$, $\kappa_2 = 0$, $k_0 = 0$. Then we approximately compute the value of k_1, k_2 and $\lambda_{\hat{J}}$ numerically by selecting a group of points sufficiently dense and properly distributed in the compact sets. For example, the value of $\lambda_{\hat{J}}$ defined in (45) is computed in a neighborhood of the steady-state state. Specifically, we take points for each element of $z = \mathrm{col}(z_1, \ldots, z_5) \in \mathbb{R}^{10}$ for every 0.5 such that $e \in \mathcal{Q}_{r^*}$, take points for each element of q for every $q \in \mathbb{Q}_\epsilon$, and take points for each element of $\hat{a}$ for every 0.2 such that $\hat{a} \in \mathbb{A}$. Then, by sequentially calculating the minimum eigenvalue of $D_z^T \overline{B}^T J(q, \hat{a}) J^T(q, \hat{a}) \overline{B} D_z$ for all the points, we can approximate that $\lambda_{\hat{J}} = 0.5$. Similarly, we can estimate that $k_1 = 7$, $k_2 = 160$, $K_P^* = 360$ by applying this grid method. Therefore, the controller parameters can be chosen as follows: $\alpha = 0.02$, $K_P = 800$ and $K_D = 180$.

We run the simulation for 30 seconds until the formation converges and the simulation results are shown in Figures 4 to 7. The trajectories and formation pattern of the manipulators' end-effector as presented in Fig. 4. Fig. 5 shows that the inner distance errors converge to zero as expected. Fig. 6 shows the evaluation of kinematic parameter estimates. From Fig. 7, where the joint positions and velocities are plotted, we can conclude that the end-effectors remain stationary once they reach the intended shape, e.g., they do not exhibit undesirable group motion.

B. End-effectors formation in 3D

This subsection provides simulation results using $N = 4$ Philips Experimental Robot Arms (PERA) in 3D space. As depicted in Fig. 8, the PERA has seven DOF, and its dynamic model and Denavit-Hartenberg representation can be found in [30, Appendix A]. The desired shape is a tetrahedron with slide length of 0.4 m. The incidence matrix is

$$B = \begin{bmatrix} 1 & 1 & -1 & 1 & 0 & 0 \\ -1 & 0 & 0 & 0 & 0 & 1 \\ 0 & -1 & 1 & 0 & 0 & -1 \\ 0 & 0 & 0 & -1 & -1 & -1 \end{bmatrix}.$$

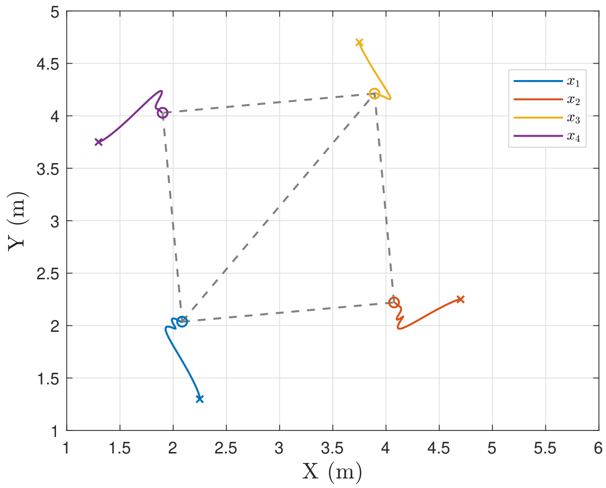

Fig. 4. Trajectories of the manipulator end-effectors from the initial positions ($\times$) to the final positions ($\circ$) in 2D space (adaptive Jacobian approach (50)).

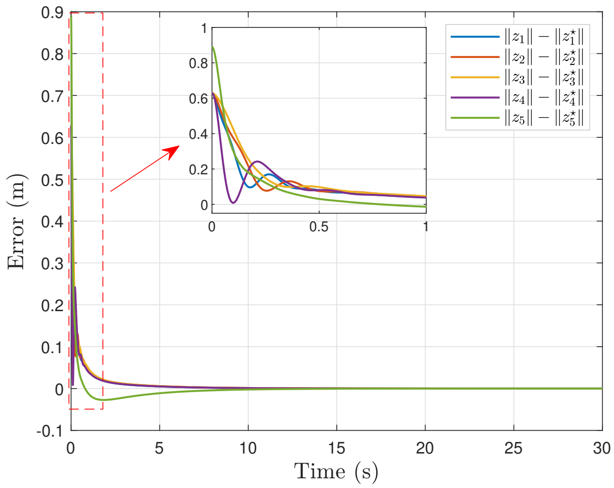

Fig. 5. Performance of the inner distance error in 2D space (adaptive Jacobian approach (50)).

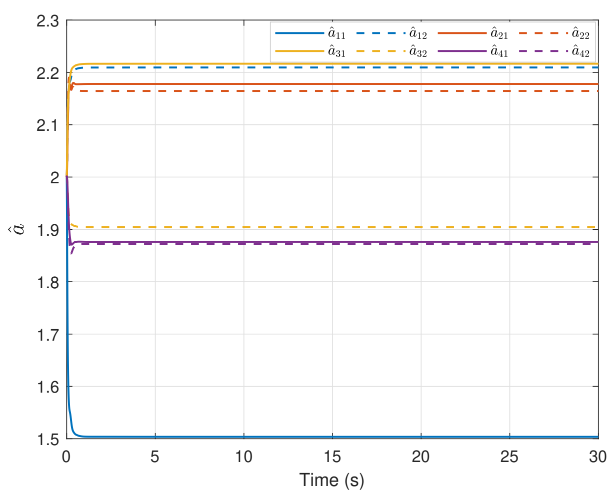

Fig. 6. Kinematic parameter estimates $\hat{a}_i(t)$, $i = 1, \ldots, 4$ in 2D space (adaptive Jacobian approach (50)).

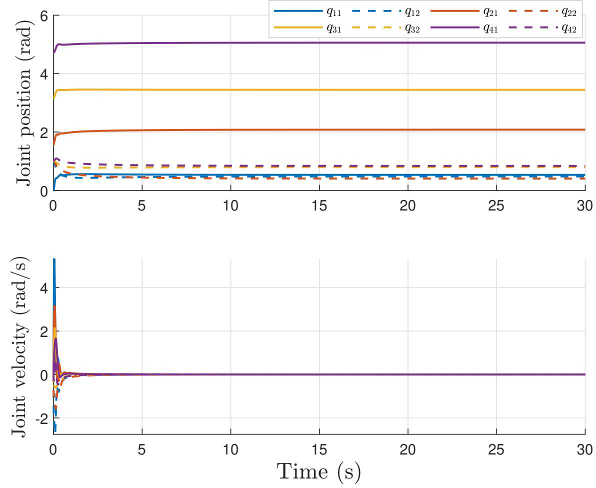

Fig. 7. Performance of joint trajectories and velocities in 2D space (adaptive Jacobian approach (50)).

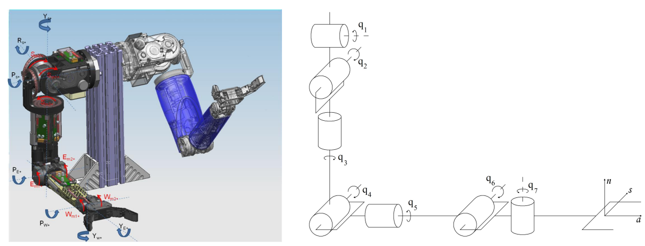

Fig. 8. Left: Graphical representation of the PERA [29]. Right: Denavit-Hartenberg representation of the PERA [30].

The bases of the 4 manipulators are located at $(0, 0)$, $(0.5, 0)$, $(0.5, 0.5)$ and $(0, 0.5)$, respectively. Using the distributed formation control as presented in Theorem 4.1, and following the parameter estimation method in the previous example, we set the controller parameters as follows: $\alpha = 0.01$, $K_P = 120$, $K_I = 1$ and $K_D = 20$.

Based on this simulation setup, we run the simulation for 50 seconds until the formation converges and the simulation results are shown in Figures 9 to 12. The trajectories and formation pattern of the manipulators' end-effector as presented in Fig. 9. Fig. 10 shows that the inner distance errors converge to zero as expected. Fig. 11 the evaluation of kinematic parameter estimates. From Fig. 12, where the joint positions and velocities are plotted, we can conclude that the end-effectors remain stationary once they reach the intended shape, e.g., they do not exhibit undesirable group motion.

VII. Conclusion

We have presented and analyzed gradient descent-based distributed formation controllers for end-effectors. By introducing an extra integrator and an adaptive estimator for gravitational compensation and stabilization, respectively, we extend the proposed gradient-based design to the case where the manipulator kinematic and dynamic parameters are not exactly known. The efficacy of the proposed methods is shown in simulation.

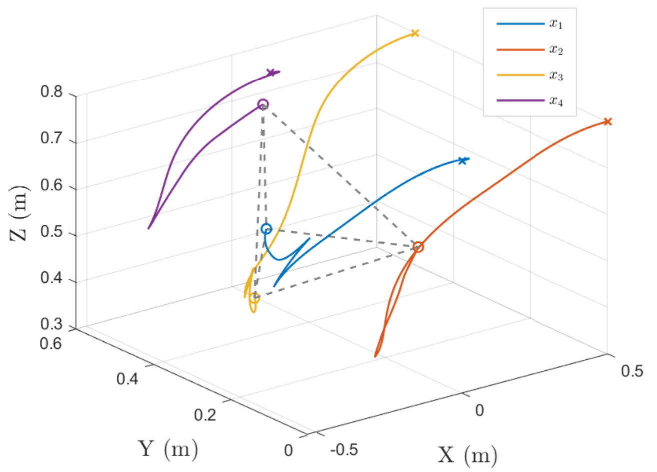

Fig. 9. Trajectories of the manipulator end-effectors from the initial positions ($\times$) to the final positions ($\circ$) in 3D space (adaptive Jacobian approach (40)).

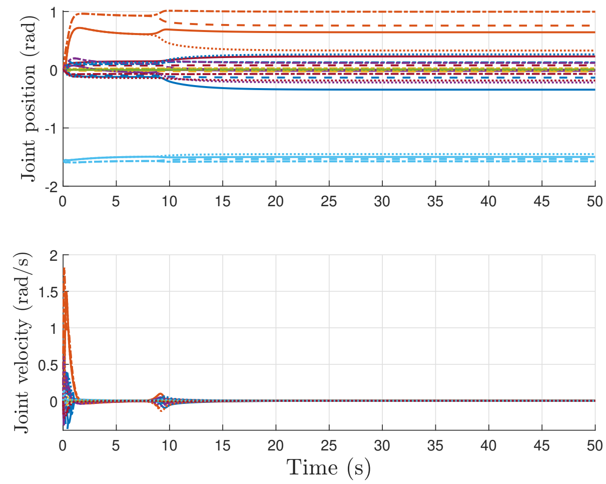

Fig. 12. Performance of joint trajectories and velocities in 3D space (adaptive Jacobian approach (40)).

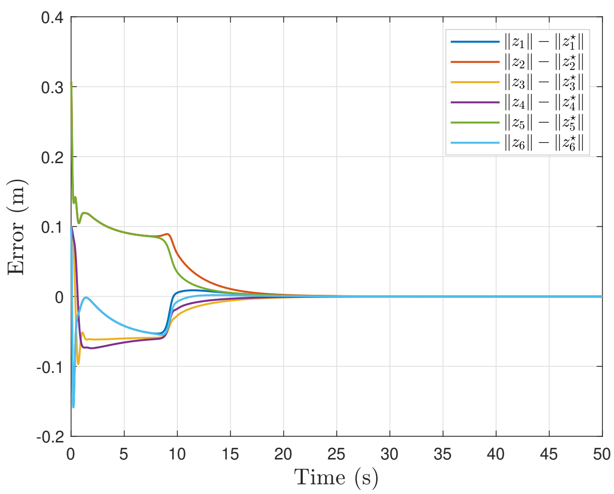

Fig. 10. Performance of the inner distance error in 3D space (adaptive Jacobian approach (40)).

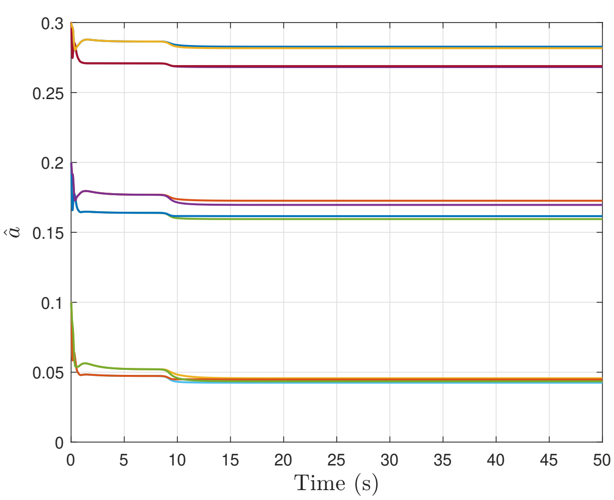

Fig. 11. Kinematic parameter estimates in 3D space (adaptive Jacobian approach (40)).

Appendix A
Proof of Proposition 3.2

Consider the closed-loop system (17). The proof is done based on a Lyapunov's direct method.

Let us begin with defining a Lyapunov function candidate $V_0(t, e, \xi)$ by

$$V_0(t,e,\xi) = \frac{1}{4}e^T(K_P + \alpha K_D)e + \frac{1}{2}\xi^T H(q(t),w)\xi + \alpha \widehat{e}^T J(q(t),a)H(q(t),w)\xi \quad (51)$$

where α is a positive constant to be determined later in (54).

The remaining proof is divided into three parts as follows.

Part 1. Let us show that V_0 is a locally positive definite function (uniformly on the exosignal $q(t)$ satisfying the joint displacement constraints).

We first note some useful properties of matrix $D_z^T\overline{B^T B}D_z$ that will be useful for subsequent analysis. As noted in [27], [6], for minimally rigid shapes, $z_l^T z_n, (l,n) \in \mathcal{E}$ can be written as a function of e. It follows that there is a smooth matrix-valued function $Q(e)$ such that $D_z^T\overline{B^T B}D_z = Q(e)$. For infinitesimally and minimally rigid graph, $D_z^T\overline{B^T B}D_z$ is full rank. Then we have $Q(0)$ is positive definite. Moreover, by continuity, there is a neighborhood of $e = 0$ with radius $r_0^* > 0$ such that, for all $e : \|e\|^2 \leq r_0^*$, $Q(e)$ is positive definite.

By using $\widehat{e} = 2\overline{B}D_z e$, the cross term of (51) satisfies

$$\begin{aligned}\alpha\widehat{e}^T J(q,a)H(q,w)\xi &\leq \alpha\|2\overline{B}D_z e\|\|J(q,a)\|\|H(q,w)\|\|\xi\| \\ &\leq 2\alpha c_{\max} c_J \|\overline{B}D_z e\|\|\xi\|\end{aligned}$$

where $c_J > 0$ is a constant satisfying $\|J(q,a)\| \leq c_J$. Applying Young's inequality to the above, we further have

$$\begin{aligned}2\alpha c_{\max} c_J\|\overline{B}D_z e\|\|\xi\| &\leq \alpha c_{\max}(2c_J^2 e^T D_z^T \overline{B^T B} D_z e + \frac{\|\xi\|^2}{2}) \\ &\leq \alpha c_{\max}(2c_J^2 Q(e)\|e\|^2 + \frac{\|\xi\|^2}{2}). \quad (52)\end{aligned}$$

Then, using (52) and **P1**, it follows that

$$\underline{\rho}_\alpha(e)\|e\|^2 + \underline{c}_\alpha\|\xi\|^2 \leq V_0(t,e,\xi) \leq \bar{\rho}_\alpha(e)\|e\|^2 + \bar{c}_\alpha\|\xi\|^2$$

for all $t \geq 0$ (i.e., all $q(t) \in \mathbb{R}^{nN}$) and all $(e, \xi) \in \mathbb{R}^{l|\mathcal{E}|} \times \mathbb{R}^{nN}$, where

$$\begin{aligned} \underline{\rho}_\alpha(e) &= \frac{1}{4}(K_P + \alpha K_D) - 2\alpha c_{\max} c_J^2 Q(e) \\ \bar{\rho}_\alpha(e) &= \frac{1}{4}(K_P + \alpha K_D) + 2\alpha c_{\max} c_J^2 Q(e) \\ \underline{c}_\alpha &= \frac{1}{2}c_{\min} - \frac{1}{2}\alpha c_{\max} \\ \bar{c}_\alpha &= \frac{1}{2}c_{\max} + \frac{1}{2}\alpha c_{\max}. \end{aligned} \tag{53}$$

Choose $r_c > 0$ such that $r_c \leq r_0^*$. Define a set $\mathcal{Q}_r$ by

$$\mathcal{Q}_{r_c} := \{e \in \mathbb{R}^{l|\mathcal{E}|} : \|e\|^2 \leq r_c\}.$$

Let $\lambda_1 := \max_{e \in \mathcal{Q}_{r_c}} \lambda_{\max}\{Q(e)\}$. Then $V_0(t, e, \xi)$ can be made locally positive definite by the following steps:

1) Choose a sufficiently small positive constant α such that

$$0 < \alpha < \alpha^* \quad \text{with} \quad \alpha^* = \frac{c_{\min}}{c_{\max}}. \tag{54}$$

2) Choose constant K_D such that $K_D > 0$.
3) Choose constant K_P such that

$$K_P > K_P^* \quad \text{with} \quad K_P^* = 8\alpha c_{\max} c_J^2 \lambda_1.$$

Then, we obtain

$$c_{01}\|e\|^2 + c_{02}\|\xi\|^2 \leq V_0(t, e, \xi) \leq c_{03}\|e\|^2 + c_{04}\|\xi\|^2 \tag{55}$$

for all $t \geq 0$, all $e \in \mathcal{Q}_{r_c}$ and all $\xi \in \mathbb{R}^{nN}$, where constants $c_{01}, c_{02}, c_{03}, c_{04} > 0$.

Part 2. This part is to show that the time derivative of (51) is negative definite (uniformly with respect to t). By calculating the time derivative of (51), we obtain that

$$\begin{aligned} \dot{V}_0|_{(17)} &= e^T(K_P + \alpha K_D)D_z^T \overline{B}^T J(q(t), a)\xi \\ &\quad + \xi^T \Big[- K_P J^T(q(t), a)\widehat{e} - K_D\xi - C(q(t), \xi, w)\xi \Big] \\ &\quad + \frac{1}{2}\xi^T \dot{H}(q(t), w)\xi + \alpha \dot{\widehat{e}}^T J(q, a)H(q(t), w)\xi \\ &\quad + \alpha \widehat{e}^T J(q(t), a)\Big[- K_P J^T(q(t), a)\widehat{e} - K_D\xi \\ &\qquad - C(q(t), \xi, w)\xi\Big] + \alpha \widehat{e}^T \dot{J}(q(t), a)H(q(t), w)\xi \\ &\qquad + \alpha \widehat{e}^T J(q(t), a)\dot{H}(q(t), w)\xi \end{aligned} \tag{56}$$

where

$$\begin{aligned} \dot{\widehat{e}} &= 2\overline{B}D_{(\overline{B}^T J(q(t), a)\xi)} e + 4\overline{B}D_z D_z^T \overline{B}^T J(q(t), a)\xi \\ \dot{J}(q(t), a) &= \sum_{i=1}^{N}\sum_{j=1}^{n} \frac{\partial J}{\partial q_{ij}}\xi_{ij} \\ \dot{H}(q(t), w) &= C(q(t), \xi, w) + C^T(q(t), \xi, w). \end{aligned} \tag{57}$$

Note that the last equality is due to property **P2**. Using (13) and removing common terms in (56), we can rewrite (56) as

$$\begin{aligned} \dot{V}_0|_{(17)} &= -\alpha \widehat{e}^T J(q(t), a)K_P J^T(q(t), a)\widehat{e} - \xi^T K_D \xi \\ &\quad + \alpha\phi(t, e, \xi, w) \end{aligned} \tag{58}$$

where

$$\begin{aligned} \phi(t, e, \xi, w) &= \dot{\widehat{e}}^T J(q(t), a)H(q(t), w)\xi \\ &\quad + \widehat{e}^T \dot{J}(q(t), a)H(q(t), w)\xi \\ &\quad + \widehat{e}^T J(q(t), a)C^T(q(t), \xi, w)\xi. \end{aligned} \tag{59}$$

It can be shown that $\phi(t, e, \xi, w)$ is a smooth function satisfying $\phi(t, 0, 0, w) = 0$ for all $q(t) \in \mathbb{R}^{nN}$ and all $w \in \mathbb{W}$. There are positive constants k_{11} and k_{12} such that

$$\|\phi(t, e, \xi, w)\| \leq k_{11}\|e\|^2 + k_{12}\|\xi\|^2 \tag{60}$$

for all $t \geq 0$, all $\|e\|^2 \leq r_c$, all $\|\xi\|^2 \leq r_c$, and all $w \in \mathbb{W}$. Let

$$\lambda_J := \min_{e \in \mathcal{Q}_{r_c}, q \in \mathbb{Q}_\epsilon, w \in \mathbb{W}} \lambda_{\min}\{D_z^T \overline{B}^T J(q, a)J^T(q, a)\overline{B}D_z\}.$$

Then, by using $\widehat{e} = 2\overline{B}D_z e$ and (60), the time derivative of V_0 defined in (58) satisfies

$$\begin{aligned} \dot{V}_0|_{(17)} &\leq \alpha(k_{11}\|e\|^2 + k_{12}\|\xi\|^2) - 4\alpha K_P \lambda_J \|e\|^2 - K_D\|\xi\|^2 \\ &\leq -\alpha(4\lambda_J K_P - k_{11})\|e\|^2 - (K_D - \alpha k_{12})\|\xi\|^2. \end{aligned}$$

Hence, for any $\alpha > 0$, the above time derivative can be made negative by the following steps:

1) Choose constant K_D such that $K_D - \alpha k_{12} > 1$.
2) Choose constant K_P such that $\alpha(4\lambda_J K_P - k_{11}) > 1$.

Finally, we obtain

$$\dot{V}_0|_{(17)} \leq -\|e\|^2 - \|\xi\|^2 \tag{61}$$

for all $t \geq 0, \|e\|^2 \leq r_c, \|\xi\|^2 \leq r_c$.

To sum up, let $K_{P,\min} = (\alpha k_{11} + 1)/(8\alpha\lambda_J)$, $K_{D,\min} = \max\{4c_{\max}c_J^2\lambda_1, \alpha k_{12} + 1\}$. Then from the proofs in *Part 1 & 2*, we can concluded that, for all $K_P > K_{P,\min}$ and $K_D > K_{D,\min}$, $V_0(t, e, \xi)$ in (51) is locally positive definite and its time derivative along (17) is locally negative definite.

Part 3. This part is to show the stability of system (17). The analysis of the convergence of the final positions of the end-effectors is similar to that in the proof of Proposition 4.1. Therefore, by using [28, Theorem 4.10], the closed-loop system (17) is locally exponentially stability at $(e, \xi) = (\mathbf{0}, \mathbf{0})$. The proof is complete.

Appendix B
Proof of Lemma 4.1

Using storage function

$$V_\eta(\tilde{\eta}) = \frac{1}{2}\tilde{\eta}^T K_I^{-1}\tilde{\eta} \tag{62}$$

it follows immediately that

$$\begin{aligned} \dot{V}_\eta|_{(22)} &= -\tilde{\eta}^T\tilde{\eta} + \tilde{\eta}^T\Big[- H(q, w)\xi - K_I^{-1}C^T(q, \xi, w)\xi \\ &\qquad + K_I^{-1}G(q, w) - K_I^{-1}G(q^*, w)\Big] \\ &\leq -\frac{1}{2}\|\tilde{\eta}\|^2 + \frac{1}{2}\Big\| - H(q, w)\xi - K_I^{-1}C^T(q, \xi, w)\xi \\ &\qquad + K_I^{-1}G(q, w) - K_I^{-1}G(q^*, w)\Big\|^2. \end{aligned} \tag{63}$$

For the above, there are constants $c_{\max}, k_c, k_g > 0$, such that $\|H(q, w)\| \leq c_{\max}$, $\|C(q, \xi, w)\| \leq k_c\|\xi\|$ and $\|G(q, w) -$

$G(q^*,w)\| \leq k_g\|e\|$ for all $q,\xi \in \mathbb{R}^{nN}$ and all $w \in \mathbb{W}$. Then (63) satisfies

$$\dot{V}_\eta|_{(22)} \leq -\frac{1}{2}\|\tilde{\eta}\|^2 + (c_{\max}^2 + K_I^{-1}k_c\|\xi\|)^2\|\xi\|^2 + (K_I^{-1}k_g)^2\|e\|^2 \tag{64}$$

which confirms (24) with $\kappa_0 = \frac{1}{2}$, $\varphi_1(s) = (K_I^{-1}k_g)^2 s^2$, $\varphi_2(s) = (c_{\max}^2 + K_I^{-1}k_c s)^2 s^2$. Moreover, for all $s : s^2 \leq r_1^*$, functions φ_1 and φ_2 satisfy $\varphi_1(s) \leq \kappa_1 s^2$, $\varphi_2(s) \leq \kappa_2 s^2$ for constants $\kappa_1 = (K_I^{-1}k_g)^2$, $\kappa_2 = (c_{\max}^2 + K_I^{-1}k_c r_1^*)^2$.

Appendix C
Proof of Lemma 4.2

Recall $V_0(t,e,\xi)$ in (51). Let us define a Lyapunov function candidate $U_1(t,e,\xi)$ by

$$U_1(t,e,\xi) = \frac{1}{4}e^T(K_P + \alpha K_D)e + \frac{1}{2}\xi^T H(q(t),w)\xi + \alpha\hat{e}^T J(q(t),a)H(q(t),w)\xi \tag{65}$$

where positive constant α satisfies (54).

Then, following the calculation in Appendix A, it is direct to derive the expressions in (29) with functions W_1, W_2 satisfy (55), and

$$\begin{aligned}\phi_\alpha(t,\tilde{\eta},e,\xi,w) &= \left[\xi^T + \alpha\hat{e}^T J(q,a)\right]\bar{f}(t,\tilde{\eta},e,\xi,w) + \alpha\phi(t,e,\xi,w)\\ \bar{f}(t,\tilde{\eta},e,\xi,w) &= f(t,\tilde{\eta},e,\xi,w) + C(q,\xi,w)\xi\end{aligned} \tag{66}$$

where $f(t,\tilde{\eta},e,\xi,w)$ and $\phi(t,e,\xi,w)$ are given by (28) and (59), respectively. Note that $\phi_\alpha(t,\tilde{\eta},e,\xi,w)$ is a smooth function satisfying $\phi_\alpha(t,0,0,0,w) = 0$ for all $t \geq 0$ and $w \in \mathbb{W}$, and inequality (30) can be confirmed by applying [31, Lemma 7.8]. More specifically, the upper bound of function ϕ_α can be computed as follows:

$$\phi_\alpha(t,\tilde{\eta},e,\xi,w) \leq \frac{1}{2}\|\xi\|^2 + \frac{1}{2}\alpha\|J^T(q,a)\hat{e}\|^2 + \alpha\|\bar{f}(t,\tilde{\eta},e,\xi,w)\|^2 + \alpha\phi(t,e,\xi,w).$$

To further derive inequality (30), We present the following growth conditions:

- By using $\hat{e} = 2\overline{B}D_z e$, $\phi(t,e,\xi,w)$ given in (59) satisfies

$$\begin{aligned}\phi(t,e,\xi,w) = {} & 2e^T \underbrace{D_z^T\overline{B}^T J(q,a)H(q,w)}_{f_1(q,\xi,w)}\xi\\ & + 4\xi^T \underbrace{J^T(q,a)\overline{B}D_z D_z^T\overline{B}^T J(q,a)H(q,w)}_{f_2(q,e,w)}\xi\\ & + 2e^T \underbrace{D_z^T\overline{B}^T \dot{J}(q,a)H(q,w)}_{f_3(q,e,w)}\xi\\ & + 2e^T \underbrace{D_z^T\overline{B}^T J(q,a)C^T(q,\xi,w)}_{f_4(q,e,\xi,w)}\xi\end{aligned}$$

  where $\dot{z} = \overline{B}^T J(q,a)\xi$, and $\dot{J}(q,a)$ is defined in (57). Let β_1, β_2, β_3 and β_4 be the maximum induced 2-norm for functions f_1, f_2, f_3 and f_4 considering all the (e,ξ,q,w) such that $\|e\|^2 \leq r_2^*, \|\xi\|^2 \leq r_2^*, q \in \mathbb{Q}_\epsilon, w \in \mathbb{W}$, respectively. Hence, by applying Young's inequality to the cross terms in ϕ, we have

$$\|\phi(t,e,\xi,w)\| \leq k_{11}\|e\|^2 + k_{12}\|\xi\|^2$$

  with $k_{11} = \beta_1 + \beta_3 + \beta_4$ and $k_{12} = \beta_1 + 4\beta_2 + \beta_3 + \beta_4$.
- By (28) and (66), we can rewrite function $\bar{f}$ as follows

$$\bar{f}(t,\tilde{\eta},e,\xi,w) = K_I\tilde{\eta} + K_I H(q,w)\xi + K_I\eta^* - G(q,w).$$

  By using the inequalities $(a+b+c)^2 \leq 3a^2 + 3b^2 + 3c^2$ for all $a,b,c \in \mathbb{R}$, and $\|K_I\eta^* - G(q,w)\| = \|G(q^*,w) - G(q,w)\| \leq k_g\|e\|$ for all $q \in \mathbb{R}^{nN}, w \in \mathbb{W}$, we have

$$\|\bar{f}(t,\tilde{\eta},e,\xi,w)\|^2 \leq k_{20}\|\tilde{\eta}\|^2 + k_{21}\|e\|^2 + k_{22}\|\xi\|^2$$

  with $k_{20} = 3K_I^2$, $k_{21} = 3k_g^2$ and $k_{22} = 3K_I^2 c_{\max}^2$, for all $t \geq 0$ and all $(\tilde{\eta},e,\xi,w)$.
- Let β_5 be the maximum induced 2-norm for function $D_z^T\overline{B}^T J(q,a)J^T(q,a)\overline{B}D_z$ for all $e : \|e\|^2 \leq r_2^*, q \in \mathbb{Q}_\epsilon, w \in \mathbb{W}$. Then, we have,

$$\frac{1}{2}\alpha\|J^T(q,a)\hat{e}\|^2 \leq 2\alpha\beta_5\|e\|^2.$$

Hence, it can be verified that the defined function ϕ_α is locally quadratic satisfying

$$\phi_\alpha(t,\tilde{\eta},e,\xi,w) \leq k_0\|\tilde{\eta}\|^2 + k_1\|e\|^2 + k_2\|\xi\|^2$$

for all $t \geq 0, \|e\|^2 \leq r_2^*, \|\xi\|^2 \leq r_2^*, \tilde{\eta} \in \mathbb{R}^{nN}, w \in \mathbb{W}$, with $k_0 = \alpha k_{20}$, $k_1 = 2\alpha\beta_5 + \alpha k_{11} + \alpha k_{21}$, and $k_2 = \frac{1}{2} + \alpha k_{12} + \alpha k_{22}$.

Finally, the verification of the second and third items of Lemma 4.2 is straightforward from that the eigenvalues of a matrix are continuous functions of their entries. The fact that $D_z^T\overline{B^T}\overline{B}D_z$ can be expressed as a smooth function of e has been proved in *Part 1* of Appendix A. The proof is complete.

References

[1] H. G. de Marina, *Distributed Formation Control for Autonomous Robots*. Groningen, Netherlands: University of Groningen, 2016.
[2] K.-K. Oh, M.-C. Park, and H.-S. Ahn, "A survey of multi-agent formation control," *Automatica*, vol. 53, pp. 424–440, 2015.
[3] N. Chan, B. Jayawardhana, and H. G. de Marina, "Angle-constrained formation control for circular mobile robots," *IEEE Control Systems Letters*, vol. 5, no. 1, pp. 109–114, 2021.
[4] K.-K. Oh and H.-S. Ahn, "Distance-based undirected formations of single-integrator and double-integrator modeled agents in n-dimensional space," *International Journal of Robust and Nonlinear Control*, vol. 24, no. 12, pp. 1809–1820, 2014.
[5] H. G. de Marina, M. Cao, and B. Jayawardhana, "Controlling rigid formations of mobile agents under inconsistent measurements," *IEEE Transactions on Robotics*, vol. 31, no. 1, pp. 31–39, 2015.
[6] H. G. de Marina, B. Jayawardhana, and M. Cao, "Taming mismatches in inter-agent distances for the formation-motion control of second-order agents," *IEEE Transactions on Automatic Control*, vol. 63, no. 2, pp. 449–462, 2018.
[7] S. Zhao and D. Zelazo, "Bearing rigidity and almost global bearing-only formation stabilization," *IEEE Transactions on Automatic Control*, vol. 61, no. 5, pp. 1255–1268, 2015.
[8] M. Jafarian, E. Vos, C. De Persis, J. M. A. Scherpen, and A. van der Schaft, "Disturbance rejection in formation keeping control of nonholonomic wheeled robots," *International Journal of Robust and Nonlinear Control*, vol. 26, no. 15, pp. 3344–3362, 2016.
[9] E. Vos, A. J. van der Schaft, and J. M. A. Scherpen, "Formation control and velocity tracking for a group of nonholonomic wheeled robots," *IEEE Transactions on Automatic Control*, vol. 61, no. 9, pp. 2702–2707, 2016.

[10] D. P. Scharf, F. Y. Hadaegh, and S. R. Ploen, "A survey of spacecraft formation flying guidance and control (part I): Guidance," in *Proceedings of the 2004 American control conference*, 2003, pp. 1733–1739.
[11] ——, "A survey of spacecraft formation flying guidance and control (part II): Control," in *Proceedings of the 2004 American control conference*, 2004, pp. 2976–2985.
[12] D. Xu, X. Wang, Y. Su, and D. Wang, "Formation control in dynamic positioning of multiple offshore vessels via cooperative robust output regulation," in *2017 IEEE 56th Annual Conference on Decision and Control (CDC)*. IEEE, 2017, pp. 4070–4075.
[13] J. J. E. Slotine and W. Li, *Applied Nonlinear Control*. Englewood Cliffs, NJ: Prentice hall, 1991.
[14] R. M. Murray, Z. Li, and S. S. Sastry, *A Mathematical Introduction to Robotic Manipulation*. CRC press, 1994.
[15] M. W. Spong, S. Hutchinson, and M. Vidyasagar, *Robot Modeling and Control*. New York: Wiley, 2006.
[16] R. Ortega, A. Loría, P. J. Nicklasson, and H. Sira-Ramírez, *Passivity-based Control of Euler-Lagrange Systems: Mechanical, Electrical and Electromechanical Applications*. Springer Science & Business Media, 1998.
[17] R. Kelly, V. S. Davila, and A. Loría, *Control of Robot Manipulators in Joint Space*. Springer Science & Business Media, 2005.
[18] H. G. de Marina, "Maneuvering and robustness issues in undirected displacement-consensus-based formation control," *arXiv preprint arXiv:2008.03544*, 2020.
[19] H. G. de Marina, B. Jayawardhana, and M. Cao, "Distributed rotational and translational maneuvering of rigid formations and their applications," *IEEE Transactions on Robotics*, vol. 32, no. 3, pp. 684–697, 2016.
[20] B. D. O. Anderson, C. Yu, B. Fidan, and J. Hendrickx, "Rigid graph control architectures for autonomous formations," *IEEE Control Systems Magazine*, vol. 28, pp. 48–63, 2008.
[21] H. Wu, B. Jayawardhana, H. Garcia de Marina, and D. Xu, "Distributed formation control of manipulators' end-effector with internal model-based disturbance rejection," *arXiv preprint arXiv:2103.14595*, 2021.
[22] A. van der Schaft and D. Jeltsema, "Port-Hamiltonian systems theory: An introductory overview," *Foundations and Trends in Systems and Control*, vol. 1, no. 2-3, pp. 173–378, 2014.
[23] C. C. Cheah, S. Kawamura, S. Arimoto, and K. Lee, "PID control of robotic manipulator with uncertain Jacobian matrix," in *Proceedings 1999 IEEE International Conference on Robotics and Automation (ICRA)*. IEEE, 1999, pp. 494–499.
[24] C. C. Cheah, M. Hirano, S. Kawamura, and S. Arimoto, "Approximate jacobian control for robots with uncertain kinematics and dynamics," *IEEE Transactions on Robotics and Automation*, vol. 19, no. 4, pp. 692–702, 2003.
[25] W. E. Dixon, "Adaptive regulation of amplitude limited robot manipulators with uncertain kinematics and dynamics," *IEEE Transactions on Automatic Control*, vol. 52, no. 3, pp. 488–493, 2007.
[26] H. K. Khalil, *High-Gain Observers in Nonlinear Feedback Control*. Philadelphia: SIAM, 2017.
[27] S. Mou, M. A. Belabbas, A. S. Morse, Z. Sun, and B. D. O. Anderson, "Undirected rigid formations are problematic," *IEEE Transactions on Automatic Control*, vol. 61, no. 10, pp. 2821–2836, 2016.
[28] H. K. Khalil, *Nonlinear Systems*, 3rd ed. New Jersey: Prentice Hall, 2002.
[29] R. Rijs, R. Beekmans, S. Izmit, and D. Bemelmans, *Philips Experimental Robot Arm: User Instructor Manual*, Koninklijke Philips Electronics N.V., Eindhoven, The Netherlands, 2010.
[30] M. Munoz-Arias, "Energy-based control design for mechanical systems: Applications of the port-hamiltonian approach," Ph.D. dissertation, University of Groningen, The Netherlands, 2015.
[31] J. Huang, *Nonlinear Output Regulation: Theory and Applications*. Philadelphia: SIAM, 2004.

Haiwen Wu received the B.Sc. degree in automatic control from Nanjing University of Science and Technology, China, in 2014. He is currently with the Faculty of Science and Engineering, University of Groningen, The Netherlands, working toward his Ph.D. degree. His research interest includes nonlinear control, output regulation, and robotic systems.

Bayu Jayawardhana (SM'13) received the B.Sc. degree in electrical and electronics engineering from the Institut Teknologi Bandung, Bandung, Indonesia, in 2000, the M.Eng. degree in electrical and electronics engineering from the Nanyang Technological University, Singapore, in 2003, and the Ph.D. degree in electrical and electronics engineering from Imperial College London, London, U.K., in 2006. He is currently a professor of mechatronics and control of nonlinear systems in the Faculty of Science and Engineering, University of Groningen, The Netherlands. He was with Dept. Mathematical Sciences, Bath University, Bath, U.K., and with Manchester Interdisciplinary Biocentre, University of Manchester, Manchester, U.K. His research interests include the analysis of nonlinear systems, systems with hysteresis, mechatronics, systems and synthetic biology. Prof. Jayawardhana is a Subject Editor of the International Journal of Robust and Nonlinear Control, an Associate Editor of the European Journal of Control and a member of the Conference Editorial Board of the IEEE Control Systems Society.

Hector Garcia de Marina (M'17) received the M.Sc. degree in electronics engineering from the Complutense University of Madrid, Madrid, Spain, in 2008, the M.Sc. degree in control engineering from the University of Alcala, Alcala de Henares, Spain, in 2011, and the Ph.D. degree in systems and control from the University of Groningen, Groningen, the Netherlands, in 2016. He held a postdoctoral position in the École Nationale de l'Aviation Civile in Toulouse from 2016 to 2018. From 2018 to 2020, he was an assistant professor at the Unmanned Aerial Systems Center, University of Southern Denmark. From 2020 to 2022, he was a research fellow in the Complutense University of Madrid. Currently, he is a *Ramón y Cajal* researcher in the University of Granada. His research interests include the guidance navigation and control for autonomous robots, and multi-agent systems.

Dabo Xu received the B.Sc. degree in mathematics and applied mathematics from Qufu Normal University, China, in 2003, the M.Sc. degree in operations research and cybernetics from Northeastern University, China, in 2006, and the Ph.D. degree in automation and computer-aided engineering from The Chinese University of Hong Kong, Hong Kong, China, in 2010. He is currently a professor at School of Automation, Nanjing University of Science and Technology, China. He was a postdoctoral fellow at The Chinese University of Hong Kong and then a research associate at The University of New South Wales at Canberra, Australia. His current research focus is on nonlinear control and distributed control with their applications to modeling and control of robotic manipulators and unmanned aerial vehicles. He is a Subject Editor of the International Journal of Robust and Nonlinear Control, a member of the editorial board of Journal of Systems Science and Complexity, and an Associate Editor of Control Theory and Technology.